UNIVERSITY OF READING

Department of Meteorology

The Representation of Extreme Precipitation in the HadRM3P Regional Climate Model

A dissertation submitted in partial fulfilment of the requirement for the degree of

Master of Atmosphere, Ocean and Climate.

David Michael Hein-Griggs

18 August 2008

Abstract

Extreme precipitation is an important concern in many parts of the world due to its impacts on society in the form of agriculture effects, the ecosystem, industry, and loss of life and property. Reliable estimates of future extreme precipitation in a changing climate are a valuable guide for policy makers in determining infrastructure requirements for the 21st century.

This study examines the ability of the Hadley Centre RCM HadRM3P to simulate present-day extreme precipitation in four different climatic regions: Europe, Southern Africa, the continental USA, and South Asia. The RCM is nested within the 'quasi-observed' ECMWF ERA-40 reanalysis data set for a 42 year period (1957-1999).

The results show that HadRM3P is able to reproduce extreme precipitation in regions and/or seasons in which large scale precipitation is the main source of extreme precipitation. In these areas, the model simulates the spatial and temporal distribution of extreme precipitation relatively well, with a tendency to overestimate extreme precipitation. In most areas in which convection is the main driver of extreme precipitation, the model shows a dry bias.

Use of 3x3 spatial pooling is explored as a method of improving model performance in simulating extreme precipitation by reducing grid box noise and increasing the sample size. Spatial pooling is able to improve pattern correlation between the model and observations for all regions and seasons.

The author concludes by suggesting further research investigating alternative or improved observational data to add confidence to the results of the model validation, identifying reasons for the model biases and improving the model's performance in simulating convective rainfall.

Contents

List of Acronyms

AR4	Fourth Assessment Report of the Intergovernmental Panel on Climate Change
DJF	December-January-February
ECMWF	European Centre for Medium Range Weather Forecasting
ERA40	ECMWF re-analysis (1957-2002)
GCM	General Circulation Model
HadAM3H	Hadley Centre Atmospheric Model version 3
HadCM3	Hadley Centre Coupled Climate Model version 3
HadRM3P	Hadley Centre Regional Model version 3 (PRECIS Physics)
IPCC	Intergovernmental Panel on Climate Change
ITCZ	Inter-Tropical Convergence Zone
JJA	June-July-August
JJAS	June-July-August-September
MAM	March-April-May
ON	October-November
PRECIS	Providing Regional Climates for Impacts Studies
RCM	Regional Climate Model
RT5	Ensembles Research Theme 5 observational data set
SI	The International System of Units
SON	September-October-November
SRES	IPCC Special Report on Emissions Scenarios
SST	Sea Surface Temperature
UDP	Unified Daily Precipitation data set
UNFCCC	United Nations Framework Convention on Climate Change

Chapter 1

Introduction

Reliable projections of extreme precipitation in a changing future climate are of vital interest to planners and policymakers due to the massive impact that extreme precipitation can have on human life and property.

Climate models are the main tools for studying potential changes in extreme precipitation and other weather. Global general circulation models (GCMs) model the whole planet's atmosphere, ocean and many other processes, but lack the resolution required to reproduce small-scale weather events such as the storms associated with extreme precipitation. It is at this regional scale that extreme precipitation can directly impact human life. Dynamical downscaling from the GCM coarse resolution to a finer resolution is thus necessary to better resolve these types of small-scale weather events. This is accomplished through the use of nested regional climate models, which depend on the GCM for input data and model a region of the Earth at higher spatial and temporal resolutions than the GCM.

To increase confidence in the climate projections made by regional models, their simulation of current climate can be compared against historical weather observations to determine how well they can reproduce the climate. This process is called model validation. A thorough validation can identify deficiencies and problems within the model. This knowledge is useful in interpreting the model output and may be used to help improve the model.

In this study, the HadRM3P regional model undergoes validation with respect to its representation of extreme precipitation. HadRM3P is part of the PRECIS (Providing Regional Climates for Impacts Studies) system, developed by the Met Office Hadley Centre for Climate Change, Exeter, UK. PRECIS is a flexible regional modelling system which can be run over any area of the globe on a personal computer utilising the freely available Linux operating system.

HadRM3P is driven at its boundaries by observational re-analysis data from the ERA-40 project.

Re-analysis data can be used to provide quasi-observational boundary data as they are based on historical observations. HadRM3P is run for a 42 year duration over four different climatic regions of the Earth. These four regions (Europe, Southern Africa, the United States apart from Alaska and Hawaii (i.e. continental USA) and South Asia) have widely different processes that are responsible for extreme precipitation. Each region differs (spatially) in the location of areas within the region which experience extreme precipitation as well as (temporally) in the times of the year in which extreme precipitation occurs.

A test of the quality of HadRM3P in reproducing the spatial and temporal distribution of extreme precipitation over these four areas provides a measure of the **skill** of the model with respect to extreme precipitation. Knowledge of the model skill is useful in assessing projections of extreme precipitation from HadRM3P experiments driven by output data from a GCM in present day and future climates as it provides information which can be used in assessing model uncertainty.

1.1 Definition of Extreme Weather Events

Extreme weather events are natural phenomena that occur very rarely and represent amounts near the very maximum and minimum of the historical distribution of meteorological records. Extreme events are unusual in their intensity, often unexpected and unseasonable, and can have a severe and significant impact on society in catastrophic quantities via affects on agriculture, the ecosystem, water resources, human health, industry and infrastructure. Extreme precipitation events in the form of high amounts of rainfall can contribute to flooding, landslides and mud flows. Effects of extreme precipitation on the natural environment can often be disproportionally larger than the cumulative effect of normal precipitation patterns. The magnitude of societal impacts of extremes depends upon a variety of factors such geographic location, population density, infrastructure design standards and emergency response systems (Parry et al., 2007).

Despite the rarity of extreme weather events, they are naturally occurring events produced by the same physical processes which account for other weather events. Due to differing climates across the globe, extreme values are generally defined relative to average values over a particular climatic region at a given time rather than a uniformly quantifiable value, e.g. a daily rainfall amount that represents an extreme value over an arid region is likely an average or below average amount for a tropical area (Zhu and Toth, 2001).

1.2 Historical Trends of Extreme Precipitation

Historical observations of rainfall are useful in determining whether the increase in observed global average temperature during the latter half of the 20th century has been accompanied by increasingly frequent and intense extreme precipitation (Groisman et al., 2005). Several studies have examined historical records for evidence of such trends. Klein Tank and Können (2003) studied temperature and precipitation records from 100 meteorological stations in Europe during the period 1946-1999. They found that averaged indices of precipitation related extremes for seven different variables (a range of threshold values exceeded in precipitation amount and wet day frequency) increased during this period, albeit with low spatial coherence of the trend. Fowler and Kilsby (2003) examined the rainfall record for the UK for the period 1960-2000 and found that the magnitude of extreme rainfall (as defined by a daily rainfall amount that exceeds two standard deviations above the long term mean) had increased by twofold in some parts of the UK since 1960. Furthermore, due to increased frequency of extreme precipitation events and changes in their seasonality, one in 25 year events became one in 6 year events over the period. Using data from approximately 200 long term stations, Karl and Knight (1998) showed that total annual precipitation amount had increased over the continental United States by 7% in the period 1910-1995, due primarily to the contribution from precipitation events in the upper 10%, with the changes causing the areas of the United States affected by high precipitation events to increase.

New et al. (2006) performed a study over southern and West Africa during the period 1961-2000 focused on extremes in climate, including precipitation. They found few statistically significant and spatially consistent trends in precipitation, which they ascribed to regional rainfall being affected by differing factors in Africa such as terrain differences and differing circulation patterns. Regionally averaged daily rainfall intensity did show statistically significant increases. For South Africa, Mason et al. (1999) studied the periods 1931-1960 and 1961-1990 and identified increases in intensity of extreme rainfall events affecting approximately 70% of the country. Fauchereau et al. (2003) also identified regions of South Africa which experienced more extreme precipitation events at a daily time scale in the later decades of the century, as well as increased variability in interannual rainfall in the same period.

Roy et al. (2004) analysed daily precipitation records for India for the period of 1910 to 2000 based on 129 meteorological stations. An analysis of the trends in seven precipitation indices (annual precipitation; largest 1,5 and 30 day events; 90th, 95th and 97.5th percentile daily precipitation) at each station showed that 61% of the time series showed an upward trend, consistent with expected increases in extreme precipitation due to greenhouse gas induced warming (e.g. Frei et al., 1998).

1.3 Extremes and Risk Management

The insurance industry has a strong economic interest in estimating future changes in the intensity and frequency of extreme events, especially at the regional scale. Recent catastrophic floods in Europe in summer 2002 and in the UK (summers of 2000, 2002 and 2007) produced insurance claims costing 19 billions Euros and 4 billion Pounds Sterling, respectively (Fowler et al., 2003; Association of British Insurers, 2008). The summer of 2007 was the wettest on record, with the number of bad weather claims in June and July 2007 submitted to UK insurers the equivalent to the number of bad weather related claims over an average four year period (Association of British Insurers, 2008).

The 1990s saw a record level of storms causing damage in the USA, with costs averaging 6 billion dollars per year of that decade (Easterling et al., 2000). More recently, flooding in the upper mid-western United States in June of 2008 saw 9 of 15 major rivers in Iowa at record heights, with the flood causing losses of millions of acres of soya beans and corn and 16% of tillable soil in the state of Iowa underwater.

Many factors are at work in the economic impact of extreme events, such as increased vulnerability to extreme weather events in some areas. Climate change induced developments in extremes are one area of strong current interest. As attention is drawn to climate change related risks of flooding and mapping of flood-prone areas improves, many insurers are significantly increasing premiums or denying home insurance altogether for certain areas (Crichton, 2007). A UK government report projects the cost of flood events to increase to 30-40 times higher than current values by 2080, up to £42 billion in current rates (Evans et al., 2004).

Because of the multitude of impacts that increased extreme precipitation could cause, reliable projections of future changes in frequency, intensity, and spatial and temporal patterns for extreme precipitation under various scenarios of future atmospheric greenhouse gas levels are of vital interest for informing policy decisions on mitigation and adaptation to anthropogenic climate change (Parry et al., 2007; Ekstrom et al., 2005; Fowler et al., 2005).

1.4 Extremes in a Changing Climate

The 2007 Fourth Assessment Report of the Intergovernmental Panel on Climate Change (hereafter AR4) comprehensively assesses the current knowledge obtained through research into climate change relevant to policymakers. The AR4 Working Group II Contribution: Impacts, Adaptation and Vulnerability (Parry et al., 2007) states that extreme events are projected with a high degree of confidence to increase in frequency and intensity due to human induced

climate change. Heavy precipitation events in particular are given a likelihood of **Very Likely** (90 to 99 percent probability) to increase in frequency and intensity, leading to detrimental impacts on a variety of sectors, though this result does not apply to all regions and seasons. Furthermore, it states that changes in the frequency and intensity of extreme events are likely to have a larger immediate impact than changes in impacts due to small changes in the mean amount.

AR4 also states that extreme events are **Likely** (greater than 66% probability) to have a much greater impact on society in a warming climate. For extreme precipitation, part of this assessment (at least for middle and high latitude areas on a broad scale) is based on physical grounds in that the saturation mixing ratio, as characterised by the Clausius-Clapeyron equation, has a temperature dependence. As it warms, the maximum moisture holding capacity of the atmosphere increases. If relative humidity remains largely unchanged, and there is good observational and modelling evidence to support this, then the total amount of moisture in the atmosphere will be higher at higher temperatures. This leads to changes in the hydrological cycle and a variety of climate related feedbacks. For example, increased atmospheric temperature causes a positive feedback as increased potential for release of latent heat intensifies developing rainfall systems and provides more precipitable water (Mason and Joubert, 1994; Frei et al., 1998; Trenberth et al., 2003). This "moisture effect" varies according to local climatological features, having its strongest presence in maritime and coastal areas.

While there is not a unique definition of extreme precipitation, it is often described in terms of return periods, which is the average interval between events of the same magnitude. An urban planner, as advised by statistics on heavy precipitation and a cost-benefit analysis, may decide to construct flood defences and buildings that cope with one in ten year extreme precipitation events but not one in a hundred year extreme precipitation. In a warming climate, it is plausible that an event with a long interval return period (e.g. 1 in 20) could see the interval decrease such that it becomes a 1 in 3 or 1 in 5 year event (Huntingford et al., 2003). Presented with information about the high likelihood of increased extreme precipitation, decisions may be made to upgrade and increase flood impact sectors (dams, sewers, drainage, urban planning, building codes, etc.).

Chapter 2

Climate Modelling and Extreme Precipitation

The atmosphere-ocean system in which weather and climate are observed is constantly evolving, influenced by global factors, such as the energy the Earth receives from the sun and ocean currents that can span thousands of kilometres, as well as local factors such as the detailed physiography of the land surface. Physical experiments testing the effect on climate of (for example) changing amounts of greenhouse gas concentrations in the atmosphere would require observed multiple copies of Earth with differing concentrations of greenhouse gases for many years, conditions which are obviously not attainable. Despite our limitations, we have an ever-evolving level of scientific understanding of the physical basis of the behaviour of the atmosphere and oceans and their interaction with internal and external forcing factors. This knowledge can be represented mathematically and thus approximated by computer code. When modelled on a computer, the experiment described above becomes feasible, as the conditions of the experiment can be met in computer based simulations of the Earth. Computer models thus allow climate related experiments investigating all kinds of weather, including extreme precipitation (Ebi et al., 2003).

Climate models can simulate a multitude of meteorological processes. As a rule, precipitation is much more difficult to accurately model than large-scale meteorological processes such as surface temperature. This is due to the high temporal and spatial variability of precipitation as well as its event type nature. Both the amount and the occurrence of precipitation need to be represented in the model. Additionally, many complex processes contribute to the duration, onset, and intensification of precipitation events. Accurate simulation of precipitation in climate models remains a very challenging activity in which further improvement is needed (Dai et al., 2005; Ebert et al., 2003).

2.1 General Circulation Models

A general circulation model (GCM) is a computer-based mathematical representation of the Earth's climate system in three dimensions as it evolves in time, based on the physical properties, interactions and feedback processes of the climate. The most important physical, biological, and sometimes chemical, processes of the climate are represented. Climate models have increased in complexity over the past several decades as computers have become more powerful. Models of the main components of the climate (atmosphere, ocean, land and sea ice) have been integrated into or coupled with GCMs. Recently incorporated are atmospheric chemistry processes and the carbon cycle. Currently the resolution of the atmospheric part of a GCM is on the order of 100-300 kilometres horizontally with 20-40 vertical levels in the atmosphere.

GCMs are able capture the broad characteristics of current climate well, including the general circulation patterns, temperature and synoptic scale precipitation (Daikaru, 2006). They can represent large scale features such as the El Niño-Southern Oscillation and the Indian summer monsoon (Ashrit et al., 2001) as well as large scale changes in the climate of the recent past. Even so, many meteorological processes that impact upon a locality are too small to be adequately represented in a GCM grid box (Christensen et al., 2007; Frei et al., 2006). This is due to to the relatively coarse resolution of the GCM. Elements of the climate system that impact on finer scale meteorological processes (i.e. sub-grid scale processes, in the sense that the spatial dimensions of the process or property are smaller than the grid box dimensions), such as extreme precipitation, cannot be accounted for sufficiently (Kiktev et al., 2003).

Additionally, events such as cyclones and fronts, which are often associated with extreme precipitation, are not properly reproduced by GCMs (Hudson and Jones, 2002b). Extreme precipitation can also arise due to interaction with sub-grid scale topography not present in the GCMs, and the temporal resolution of the GCM may also be too long to capture extreme precipitation events in that these events can start and finish within a matter of minutes (Gregory and Mitchell, 1995), which is shorter than the average timestep of GCMs.

2.2 Past experiments with GCMs and intense precipitation

Gregory and Mitchell (1995) carried out an experiment comparing output from the UKHI GCM (2.5° by 3.75° horizontal resolution, 11 vertical levels) with climatologies of surface temperature and precipitation. While the GCM was in most parts within 50% of the values

in the climatologies of precipitation, the model's simulation of precipitation was identified as being deficient in many areas. The authors identified the need for higher resolution regional simulations in order to make more reliable predictions in local climatology. Hennesy et al. (1997) showed that the UKHI model and the Australian CSIRO9 model projected an increase of 10% in global average precipitation and an increase in convective rainfall at low and middle latitudes. The authors identify the model as being incapable of simulation of magnitudes and realistic daily frequencies of extreme precipitation and point to improved model formulation and higher spatial resolutions as a means of improvement. Similarly, Mason and Joubert (1994) utilised the CSIRO9 model over Southern Africa, carrying out an analysis of changes in extreme rainfall due to a doubling of atmospheric carbon dioxide. Their results suggested future increases in the frequency and intensity of extreme daily rainfall events, while the validation of the control period was very poor in areas with large topographical gradients that are the dominant determining factor in local patterns of rainfall. The authors again point to the coarse resolution of the GCM as the reason for this.

2.3 Downscaling

As computers have become more powerful, the horizontal and vertical resolutions of GCMs have indeed increased, but in many cases the extra computational resource has been used to increase the complexity of the models. Thus in general the spatial resolutions of cutting edge GCMs are still not fine enough to resolve many important weather features, including small scale precipitation. This has lead to the derivation of methods to **downscale** coarse resolution GCM data to finer scales.

2.3.1 Statistical downscaling

Statistical methods of downscaling exist to deduce fine-scale information from the GCMs (Murphy, 1999; Landman et al., 2005). Statistical downscaling requires high quality observational data for long time periods in order to try to form a robust relationship between the large scale and small scale climate components. An assumption that stable empirical relationships can be established between atmospheric processes occurring at differing temporal and spatial scales must be made, such as (for example) relationships between mesoscale weather patterns and daily rainfall patterns or evaporation amounts (Wilby et al., 1998). Statistical downscaling has its main advantage in that it is computationally inexpensive. Its drawbacks are that it requires high quality, lengthy observational data sets (which may be difficult to locate) and that the posited fine scale relationship between the large scale feature may not exist in the future (Jones

et al., 2004). Potential changes in feedbacks in a different future climate could weaken or invalidate the statistical model. Statistical and dynamical approaches to downscaling of heavy precipitation have recently been compared in the STARDEX project (Haylock et al., 2006).

2.3.2 Dynamical downscaling

The use of a regional climate model (RCM) is a method of addressing the limitations of GCMs and statistical downscaling (Giorgi, 1990). A regional climate model is a high resolution climate model covering a limited area of the surface of the earth rather than the entire surface of the earth that a GCM covers. Like GCMs, RCMs are computer based models which solve mathematical equations on a three dimensional grid based on the laws of physics as they apply to the atmosphere and climate system. RCMs depend on a GCM in that they are "nested" into a GCM or re-analysis. In this arrangement, the GCM provides boundary data input values for the RCM at the edges of the region model domain, and the resulting high resolution output data from the RCM is dynamically, physically and hydrologically consistent with the coarse resolution input data, which is not possible in statistical downscaling (Kanamitsu et al., 2008). Because of this, RCMs represent "dynamical" downscaling.

Dynamical downscaling has an advantage over statistical downscaling in that it is formulated on physical considerations and laws which remain constant.

2.4 Regional Climate Models

Regional climate models are a useful tool for analysis of climate in greater detail, especially in regions where there are significant orographic or coastline influences on the distribution of climate variables or where higher resolution of atmospheric motions or processes is important (Giorgi, 1990; Jones et al., 1995). Regional models nested into GCMs have been around since the late 1980s. They have become more complex as computer power has increased and model formulations of their parent GCMs has accounted for more climate processes.

RCMs do not replace GCMs. They are intended as tools to be used alongside a GCM in order to add fine scale detail to larger scale climate projections. RCMs can address the need for regional detail in the manner that the climate may change in the future, including changes in variability (Arnell et al., 2003) and extreme weather events (Jones and Reid, 2001; Frei et al., 2006; Buonomo et al., 2007; Kendon et al., 2008).

Because regional models only cover a limited area, they need to take information at their boundaries from the GCMs. Time dependent meteorological variables such as temperature,

winds, humidity and pressure are taken from output from a GCM or from observational analyses and then interpolated to the grid of the regional model in a buffer area surrounding the limited area domain.

2.5 Added value of RCMs

Regional models exhibit benefits over GCMs in several areas. The increased resolution allows for more accurate representation of orography, land and water contrasts and land-surface characteristics. RCMs offer significant improvement in particular for processes forced directly by topography such as orographic rainfall and monsoon circulation (Bhaskaran et al., 1996, 1998). In an area of the Earth where the terrain is flat, orographic effects on atmospheric processes are minimal. In such areas the higher resolution of the regional model may not produce results significantly different from the GCM. However, in mountainous and coastal areas, the terrain can have a large effect on production of certain meteorological phenomena such as rainfall produced by the movement of air masses over mountains. In such areas, the higher resolution of the regional model allows for the terrain to impact these events and reproduce distribution of precipitation over regions with complex topography (Jones et al., 1995; Frei et al., 2003, 2006). Even in relatively flat areas, the higher resolution of the RCM allows for the production of mesoscale features, such as cyclogenesis, which results from the ability of the RCM to resolve higher resolution atmospheric motions and correctly respond to drivers of such features such as surface latent heat release.

In keeping with this, regional models can project climate change in greater detail. The effects of increased greenhouse gases can cause warming or cooling in places that can change patterns of wind flow, which can affect the location and intensity of rainfall. The higher resolution of the regional model allows for representation of the terrain elements which impact these features.

The coarse resolution of a GCM means that the coasts and in particular smaller islands are not represented as accurately in GCM models when compared to RCMs (Figure 2.1). Smaller islands may be represented as ocean grid boxes. Because the weather over an ocean point may be quite different from weather over a land point (due to differing circulations affected by non-uniform terrain and the lower thermal inertia of land versus sea), representation of islands as ocean means that the model data which is output over small islands may not be as accurate as in the regional model, in which land points can be resolved. This is of special interest in island areas containing mountains or hills that can affect local weather.

The increased resolution of an RCM allows for it to better simulate weather extremes (Christensen et al., 2002), which are again often dependent on local surface features and circulation.

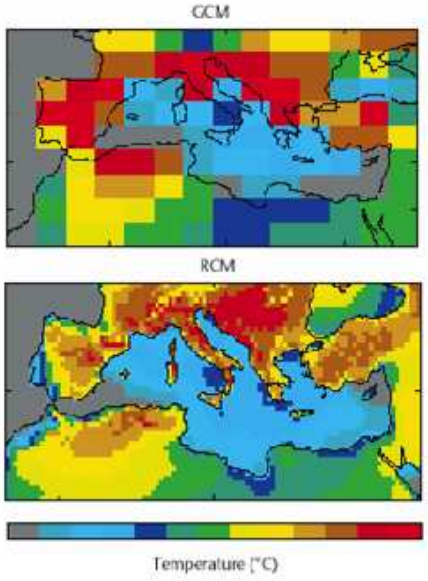

Figure 2.1: Surface temperature on the GCM grid (left) and the RCM grid (right). The RCM grid better resolves islands and coastal areas.

RCMs have been shown, via comparison of regional climate model precipitation with GCM precipitation, to produce better estimates of extreme precipitation (Jones et al., 1997; Durman et al., 2001; Christensen et al., 2002). Hurricanes and cyclones, which produce extreme weather, are able to be reproduced in regional models whereas they are not present in GCMs (Hudson and Jones, 2002b). Regional model output data is also at a high enough resolution that it can be used to drive other types of models (Salzmann et al., 2006; Lenderlink et al., 2007) which require finer scale data as inputs, such as storm surge, river and crop models.

2.6 Literature review of Regional Models and Extreme Precipitation

2.6.1 Issues in Regional Climate Modelling

In a review article, Giorgi and Mearns (1999) presented the current status of regional climate modelling at the time in a publication titled *Regional Climate Modelling: revisited*. In this paper, outstanding issues to do with regional modelling were revisited and described. Despite the problems pointed out, the authors stated that use of the one-way nesting of an RCM into a GCM is a workable solution. They stressed that the regional models need to be validated, and that one way of carrying out this validation is by running RCMs driven by observational reanalyses to verify whether the RCM simulates the regional climate successfully. This validation

1.	Numerical Nesting: mathematical formulation and strategy
2.	Spatial resolution difference between the driving data and the nested model
3.	Spin-up
4.	Update frequency of the Lateral Boundary Conditions
5.	Physical parameterisation consistencies
6.	Horizontal & vertical interpolation errors
7.	Domain size
8.	Quality of the driving data
9.	Climate drift or systematic error

Table 2.1: Denis et al. (2002) list nine potential pitfalls in use of RCMs.

with respect to extreme precipitation is an essential part of this study.

Denis et al. (2002) refers to the issues described in Giorgi and Mearns (1999) and summarises these as they relate to the utilisation of regional climate models as tools for downscaling (see Table 2.1). In this section the implications of these sources of error for the application of regional climate models to simulate extreme precipitation will be reviewed.

The experiments carried out by Denis et al. (2002) are relevant to items 1, 2, 3 and 9 of Table 2.1. The initial experiment they ran is termed the "Big-Brother" which is a high resolution RCM simulation run over a large domain to create a reference data set. This data set was then subject to filtering to remove small scale information, and that filtered data set was used to drive the same RCM at the same resolution over a smaller region contained entirely within the larger domain of the first RCM. The output from the second RCM was then compared to the unfiltered output from the first RCM to investigate the utility of the nesting technique. The model resolutions, physics, dynamics and numerics were the same, and because of this the errors produced could be ascribed to the nesting strategy utilised. Atmospheric spin-up (see section 3.3.5) was taken into consideration and analysed, as was the effect of the resolution difference between the driving data and the regional model resolution. They found that 24 hours constituted a sufficient atmospheric spin-up period. For precipitation, they reported good results apart from stationary parts of small-scale components over the ocean where stochastic convection was occurring, though they expected that to be less of an issue for longer integrations.

Sensitivity to items 7 and 8 in Table 2.1 was investigated by Jones et al. (1995) and Bhaskaran et al. (1996). Jones et al. (1995) carried out four 90-day 50km resolution RCM integrations

driven by a GCM with the same model physics. Only the domain size used differed between the four experiments. The smallest domain contained Europe, and the three successive domains each contained the area of the previous domain but were progressively larger in order to include more of the North Atlantic storm track. The purpose of this work was to carry out sensitivity tests on the domain size. Via comparison between the synoptic scale circulations of the regions with the circulations from the GCM, they found that for the two largest domains that the interior of the regional domain began to develop its own independent synoptic scale climate, one not constrained by the values in the driving GCM. Comparison of the smaller two domains with each other showed they were very similar, with the larger of the small two domains allowing less constraint by the driving data on features at finer scales. This particular domain was run for a ten year period and compared against the driving GCM and an observational climatology. They found that the spatial correlation of the RCM with climatologies of precipitation was 0.8-0.9. The RCM produced more dynamical precipitation but less convective clouds and convective precipitation, attributed to stronger vertical motion due to higher resolution. The hydrological cycle in general was intensified relative to the GCM, with the RCM producing 30% more precipitation. The authors concluded that the RCM circulation follows that of the GCM, and that errors in the RCM are inherited from the driving GCM.

In part 2 of their nested regional climate model experiments, Jones et al. (1997) compared results from model responses to doubled atmospheric carbon dioxide. An RCM and GCM with the same formulation were run for a period of ten years and then compared with each other. Once again, the RCM had an intensified hydrological cycle, with convective activity increasing in both the GCM and the RCM. The overall results of the RCM were comparable to the GCM in all seasons except summer, in which the RCM climate is less affected by the driving GCM. The authors concluded that in order to adequately capture climate variability, longer model integrations were necessary, with 30 year integrations identified as capturing 75% of the variance over Europe within this model. Finally, the authors noted that higher quality estimates provided by the RCM may result in quite different conclusions about the response of a meteorological variable to climate change than that characterised by the GCM, a conclusion which is demonstrated in particular for heavy precipitation.

Bhaskaran et al. (1996) performed a similar experiment to Jones et al. (1995) over the Indian subcontinent with the same models. Their results did not show the large sensitivity to the domain size which was found in Jones et al. (1995). This was attributed to the different climate dynamics at work in a tropical area in that synoptic scale events generated by the RCM in the tropics and subtropics are smaller amplitude waves maintained by latent heat release, while in the mid-latitudes such events are manifest as large amplitude waves associated with the mean meridional temperature gradient. The variability of the RCM exhibited a strong correlation

with the GCM on both daily and seasonal time scale, though precipitation in the RCM was again higher by 20% than the driving GCM (again attributed to stronger vertical motion in the RCM). In a follow-up paper (Bhaskaran et al. 1998), the RCM seasonal correlation was further explored in reference to the Indian summer monsoon. In regards to the intraseasonal oscillation associated with the monsoon, the RCM was shown to be influenced by the GCM on scales of 30-50 days. The enhanced resolution of the RCM allowed it to provide much greater detail in representation of monsoon precipitation, particularly in areas with topographic rainfall (with an especially strong precipitation signal in the foothills of the Himalayas).

The results of Hassell and Jones (1999) and Hudson and Jones (2002b) indicate that the higher resolution of an RCM can generate realistic short lived small scale features, such as tropical cyclones, that are absent from the GCM. These short lived features do not lead to significant deviations from the large scale mean climate of the GCM. However, they are important for accurate simulation of the local climate of parts of the region, especially for high resolution spatial or temporal details of precipitation.

Tadross et al. (2006) investigated the effects of using different physical parameterisations (item 5 of Table 2.1) in RCM runs over Southern Africa which were otherwise identical. These type of adjustments to model *physics* in order to obtain improved results are known as model *tuning*. Two different schemes for the planetary boundary layer and two different schemes for cumulus convection were employed in the MM5 RCM driven by a combination of re-analyses. In comparing model output data with observations for three different variables (precipitation, surface air temperature, number of wet days), they concluded that the simulation of the southern African climate was largely determined by the choice of these two schemes. No recommendation was made for a preferable convection scheme, and the authors identified improvement in this parameterisation as an important step towards improving modelled effects of land-surface features on local climate. This is in line with the conclusions of a number of studies which state that the parameterisations used in the regional models contain many uncertainties and require improvement (Trenberth et al., 2003), especially the parameterisation used for convection (Leung et al., 2003; Frei et al., 2006).

Noguer et al. (1998) attempted to identify the causes of systematic error in RCM runs as a method of improving quality of future RCM runs (item 9 of Table 2.1). In this experiment the error contributions of both the lateral boundary forcings and the RCM model internal physics are separately identified. Two ten year RCM integrations were carried out using the Met Office Unified Model RCM (HadRM2) driven by a GCM (HadCM2) or Met Office operational analyses and then the results compared. Analysis of surface temperature, precipitation and pressure at mean sea level was made, with errors attributed to the RCM internal physics or to the influence of lateral boundary conditions. In general, the model errors in summer were

attributed to the RCM model physics. In winter, during which the advective forcing from the boundaries was stronger, the RCM circulation and temperatures were close to the GCMs and hence errors attributed to boundary forcing.

2.6.2 Present day climates

Hudson and Jones (2002b) simulated both present day and future climate over Southern Africa using the HadRM3H regional model, which is similar to the HadRM3P model used in PRECIS, mainly differing in cloud related physical parameterisations. Two time slices were used in the study (1960-1990 and 2070-2100), with GCM output from the HadAM3H model used to drive the RCM in the control period and in the future period from a model integration run according to the IPCC SRES A2 scenario (IPCC, 2000). The primary circulation (wind driven movement of atmospheric moisture and heat) and seasonality were captured well. The hydrological cycle of the RCM was more active than in the GCM. This led to a positive rainfall bias in comparison to observations of precipitation due to excess moisture in the model, and a surface temperature cold bias attributed to greater evaporative cooling (due to increased moisture). In summer the RCM overestimated the number of rain days and the extreme rainfall was also overestimated compared to observations. In assessing the model's performance in the future, rainfall was projected to increase in equatorial regions but decrease in central and western tropical and subtropical areas.

A number of studies have attempted to assess the ability of RCMs to replicate periods of extreme precipitation in recent years. An example of this is found in Kunkel et al. (2002), in which the RegCM2 RCM was driven by the NCEP re-analysis (Kalnay et al., 1996) for the period of 1979-1988 over the continental United States. The RCM generally reproduced the interannual variability in frequency of extreme precipitation for the south, southwest, west and north central regions, with poorer agreement in the midwest and northeast. Heavy rainfall was defined by rainfall totals that exceeded amounts for 3 month, 1 year and 5 year return periods as well as by duration of precipitation events (1 day and 7 day events). Threshold amount values were calculated for these durations and return periods by identifying the largest 100 events in each grid point (in both the model results and in a gridded observational data set) and fitting them to a Gumbel distribution. The model and observational threshold amounts for the various return periods and durations were then compared to each other. For 1 day heavy precipitation events, the model threshold amounts were greater than the observational threshold amounts in the mountainous regions of the west as well as in the eastern part of the domain. For 7 day events, modelled threshold amounts in the eastern and central areas generally matched observational threshold amounts, were less than the observational threshold for the lower

Mississippi valley and higher for the western regions. While the timing of individual events did not match observations, the authors felt that the climatological frequency of modelled events was more accurate.

Anderson et al. (2003) ran a multi-model ensemble over the United States to try to reproduce the summer 1993 flooding that took place in the midwest at that time. Thirteen RCMs from various institutions worldwide were utilised and driven by the NCEP re-analysis for a period of 60 days, which spanned the peak precipitation period that was one of the causes of the flooding. All models produced positive values of overall precipitation minus evaporation, but in only two was the difference large enough to come close to observational estimates. Ten of the thirteen produced maximum precipitation values north-east of the observed location. The authors pointed out that most of the models simulated a nocturnal maximum of precipitation, which they viewed as evidence supporting the ability of RCMs to add realistic hydroclimatological detail in comparison with GCMs. The authors added, however, that much longer integrations would be needed for greater confidence in the RCM performance.

Done et al. (2005) focused on the same time period (summer 1993) to assess the performance of the WRF regional model. The WRF model used a 30km horizontal resolution and 31 atmospheric levels and was driven at the boundaries by the same NCEP re-analysis data used in Anderson et al. (2003). The length of the RCM integrated was 10 months, ending in August 1993. Sensitivity tests to the performance of the model in reference to convection scheme, land surface related model components and errors in sea surface temperatures were undertaken. WRF was found to under-predict rainfall amounts, with little difference shown in use of different convection schemes and land surface models.

Leung and Qian (2003) compared data sets arising from three sources: regional model output, re-analyses and observations over the central United States to try to reproduce flooding that occurred in summer 1993. The importance of spatial resolution was highlighted as one of the most important factors determining the quality of precipitation in the three sources. In addition to topographic enhancement that higher spatial resolution allowed for, other components of the water budget were enhanced as well by the effects of increased resolution on temperature, precipitation, clouds, radiation and more. Most of the RCMs were able to correctly simulate a nocturnal maximum of precipitation, a feature not usually reproduced in GCMs. The authors pointed to the need for longer RCM integrations to characterise with greater confidence the model skill in reproducing extreme precipitation.

Frei et al. (2003) utilised 15 year integrations (1979-1993) for four RCMs (CHRM, REMO, HIRHAM and HadRM3H) and one variable grid GCM (ARPEGE) in order to study daily rainfall amount over the Alps. All models were able to generally reproduce observed values of mean seasonal (winter, spring and autumn) and annual mean precipitation. However, in

summer all models were too dry, underestimating summer seasonal rainfall, with three (CHRM, REMO and HadRM3H) underestimating the amount by 25%. Heavy precipitation events on major mesoscale dimensions (approximately 200 kilometres) were in reasonable agreement with observations in most of the models. While the authors suggested that RCM performance in seasonal mean precipitation had improved over results from previous experiments, the summer drying in the Alpine and Mediterranean regions was identified as a task for model improvement. Deficiencies in model performance in summer precipitation are present in a number of studies (Haylock et al., 2006; Vidale et al., 2003; Hudson and Jones, 2002b).

Fowler et al. (2005) as part one of a two part study assessed HadRM3H against observational data sets with respect to extreme precipitation. Two methods of analysis were used (regional frequency analysis and individual grid box analysis). The results of their analysis suggested that HadRM3H provided a good representation of extreme rainfall for return periods of 1, 2, 5 and 10 days in most parts of the United Kingdom. In higher elevation parts of the UK, extremes were overestimated and in the eastern, leeward part of the country a too-strong "rain shadow" effect caused underestimation. In the southeast and southwest of the UK there was also underestimation of precipitation, which the authors attributed to poor representation of convection in the RCM.

Finally, the EU PRUDENCE project (Christensen et al., 2007) utilised ten RCMs driven by HadAM3H in simulations over Europe to gain information on human induced climate change and to compare several different types of model uncertainty, including uncertainty due to assumptions made by the SRES scenarios in greenhouse gas emissions levels, land surface changes and socio-political changes. In Jacob et al. (2007) the ability of the RCMs to simulate the present-day climate was assessed by comparing outputs against observational data, with focus on long term mean climate and interannual variability. The RCMs were found to reproduce the GCM circulation well. Variability of precipitation was closer to observations than surface temperature, though regional biases in the models were sometimes substantial.

2.6.3 Future climates

Many studies have been carried out in the area of changes in extreme precipitation due to human induced climate change due to its potentially catastrophic effects.

Jones and Reid (2001) used quantile and return period analysis to project changes in precipitation over Britain at the end of the 21st century. The HadRM2 RCM was driven by the HadCM2 GCM run with a compound 1% increase in carbon dioxide for a control period (1960-1990) and a future period (2080-2100). The results showed large increases in the heaviest extreme precipitation events. Both analysis methods showed increased numbers of heavy precipitation

events exceeding a fixed threshold. The greatest increases were seen in south-east England, south Wales and western Scotland.

Another study focusing on future changes to extreme rainfall was Huntingford et al. (2003). As with Jones and Reid (2001), the HadRM2 RCM was driven by HadCM2 for control and future periods. Annual maximum series of rainfall were calculated for five return periods (1, 7, 15, 30 and 60 days), and analysed using Generalised Extreme Value frequency distributions. The results showed that the nested RCM was able to simulate extreme precipitation events with good skill in the recent past. Examination of output data from the future showed a reduction in return period intervals for extreme rainfall for past values corresponding to the five chosen return periods.

Semmler and Jacob (2004) focused on extreme precipitation over Europe. The REMO 5.1 RCM was driven by HadAM3H for a 1960-1990 baseline period and a 2070-2100 future period simulated according to the SRES A2 emissions scenario. For the baseline climate, the model was able to reproduce the climatological mean precipitation well as well as return levels of daily precipitation for 10 and 20 year period. Use of 3x3 spatial pooling was used to increase reliability in calculation of return period values. For the future period, return level increases of up to 50% in parts of Europe were predicted when compared to return level amounts from the baseline climate. Additionally, return level increases of up to 100% were seen the Baltic Sea area, which the authors viewed as unrealistic and ascribed to anomalously strong SSTs in the GCM.

The study of Frei et al. (2006) utilised six RCMs for a baseline period (1960-1990) and a future period (2070-2100) driven by the same GCM (HadAM3H). The results were consistent between all RCMs, implying that the RCMs were generally well constrained by the driving GCM. Areas north of 45° N showed an increase in multi-year return values, while the southern Mediterranean region showed small changes with a general tendency towards decreases. Winter precipitation was found to increase among all RCMs with changes in extreme precipitation to be largely determined by winter seasonal mean precipitation changes. Summertime results varied between models. The study concluded that the physical formulation of the regional models contributed a great deal towards the uncertainty in climate change based extreme precipitation scenarios and that ensembles of RCMs were a way of addressing this problem.

With that same issue in mind, the EU Prudence project compared data from four GCMs and nine RCMs over Europe for a future A2 scenario (2071-2100) and control period (1961-1990). Analysis demonstrated that the summer climate was strongly influenced by the model physical formulation and high resolution processes. The spread of systematic model errors in the ensemble were compared with the spread of the climate responses in order to gain some confidence in precipitation responses. All the models showed similar results with a drying in

southern Europe (particularly in the summer) and a wetter northern Europe (particularly in winter).

Buonomo et al. (2007) ran two RCMs (HadRM2 and HadRM3H) driven by GCM output data from the HadCM2 model for a control period (1961-1990) and a future period consistent with a 1% increase per year in carbon dioxide in order to understand the importance of model formulation in changes in climate extremes. The region and boundary data used were the same as was used in the study of Murphy (2000) for intercomparison purposes. The control period was compared against a high resolution observational data set over Great Britain. Both RCMs were found to describe extreme precipitation events well over Great Britain, with HadRM3H showing better agreement with observations. For future results, a significant increase (at the 5% level) in extreme events was projected for the whole of Europe. The authors stated that increased extremes were found for some areas experiencing reduced mean precipitation, implying a future with substantial reduction in lighter precipitation events and increase in intense events as well as the conclusion that the change in mean precipitation is a poor predictor of future extremes.

2.7 Critical Analysis

Simulation of the climate is inherently difficult due to the immense complexity of the geophysical system. The processes taking place which create weather and influence climate take place on scale ranging from macro (e.g. energy from the sun reaching the whole planet) to micro (e.g. aerosol particles contributing to the formation of raindrops). Additional, the time scales involved can range from seconds to decades or longer. The complexity and chaotic nature of the climate system means a direct mathematical approach is not possible, and thus no climate model can ever be expected to be perfect in reproducing reality.

The first GCM was created in the late 1960s at the NOAA (National Oceanic and Atmospheric Administration, USA) Geophysical Fluid Dynamics Laboratory. It in itself was a breakthrough that led to better understanding of how atmospheric processes interact. Since then great strides have been made in climate modelling science. Improved numerical schemes for solving differential equations on a computer have been developed as well as improvements in schemes to reproduce sub-grid scale events. The science of meteorology has improved markedly thanks to past and ongoing research. Vastly increased computing power has allowed for climate models to take into consideration many more geophysical processes as well as increase their spatial and temporal resolutions. The same increase in computing infrastructure has allowed for multi-decade integrations to occur with ensembles of perturbed models.

The criteria for choice of reviewed publications in this study was based on their importance for improving regional modelling science in representation of extreme precipitation, with special emphasis on the four climatic regions. In reviewing the literature, a chain of important papers going all the way back to Giorgi (1990) became apparent, in which subsequent research was built upon the findings and results of previous studies as well as improved models and computing facilities.

Despite all of the improvements and ongoing research, the models remain deficient in many areas. Most of the deficiencies describing GCMs also apply to RCMs due to the similarity of their compositions. A thorough assessment of strengths and weaknesses of climate models is beyond the scope of this study. However, for the purpose of regional modelling of extreme precipitation, the main discussion points to be raised here hearken back to Table 2.1 in section 2.6.1 that lists Denis' summary of Giorgi's identified main issues in regional modelling. Some of the items in the list have been investigated thoroughly to the point that current studies do not face them with the same level of consideration as in older studies, while some of the items are still outstanding.

Item 1 in Table 2.1 deals with the model formulation and nesting strategy. This remains an outstanding issue in that climate modellers and scientists are continually active in trying to improve the models. Each new geophysical process that is represented in the model brings a whole new set of feedbacks on the other processes active in the models, and qualitatively can mean that more complex models can actually demonstrate reduced performance than older models until coding errors are identified and repaired or a better scientific understanding of the offending process is reached. The nesting strategy seems less of an area of research, though this too is being improved by modellers and new and improved schemes are being developed (Terry Davies, personal communication). In this study, the issue of model formulation is relevant to model performance in that the regional model being utilised is 8 to 10 years old. Newer regional models will share a great deal of similarity with HadRM3P, but will have the benefit of improved model formulation (though this does not necessarily mean they are "better" models).

Item 2 (spatial resolution difference between the driving data and the nested model) as well as item 4 (update frequency of the lateral boundary conditions) are issues that seem fairly settled. Denis et al. (2003) investigated the sensitivity of an RCM to the spatial differences between the RCM resolution and the resolution of the driving GCM, as well as the update frequency of the driving GCM data. They concluded that the upper limit was a factor of 12 spatially and 12 hours for the update frequency, with better performance at 6 hours. This work served to confirm the spatial difference and update frequency of driving GCM data in use by the majority of regional models at the time and since then. The values in this study

(update frequency of the GCM at six hours, spatial difference factors of 4.26 longitudinally and 2.84 latitudinally) are well within these limits described by Denis.

Item 3 (spin-up) has been investigated in a number of experiments, all of which agree that the atmosphere comes into equilibrium with the driving data within a few days while the soil data in the land surface scheme can take much longer (up to 2 years). Even so, the amount of spin-up time varies widely between the studies, and several of them do not mention discarded model spin-up at all (which does not necessarily imply that spin-up was not taken into consideration, but lacking the specific value means that the reader is left in doubt as to model performance in at least the initial year). Some studies only use a few days as spin-up, while for other the period reaches years. The amount used in this study (one model year) seems to be on the conservative side of how much data to discard, which seems a safer approach especially when modelling regions that are majority land areas (like the continental USA).

Item 5 has to do with physical parameterisation issues, i.e. the model "physics". All the geophysical processes represented in the model that are below the scale of the atmospheric dynamics must be parameterised, seeking a physically motivated statistical relationship between grid-box mean variables and effect of physical processes that are unresolved. Laprise (2008) states that some of the parameterisations in use are nothing more than crude approximations, and that parameterisations account for a large amount of the computing cost in regional modelling. For large-scale variables like surface temperature, local influences do not exert as great an effect regionally as variables that vary widely in time and space, such as precipitation. Thus the parameterisations related to clouds and precipitation are of vital importance in determining the grid box value of precipitation. For example, convective clouds are a major source of extreme rainfall, so if a model does poorly in estimating convection, it is likely to produce unrealistic precipitation. This will remain an issue in regional and global modelling until the horizontal resolution reaches a point (e.g. 1 kilometre resolution) in which convective cloud does not require parameterisation. At present, there are RCMs in use with 10 kilometre resolutions (Dankers et al., 2007) as well as numerical forecast models with 4 kilometres resolutions (e.g. The WRF model in the USA, the UK Met Office Unified Model), but 1 kilometre regional models could take years or longer to appear and be realistically usable (given the necessary requirements in computing power and storage).

Item 6 is horizontal and vertical interpolation errors. These errors seem to arise most often when mountainous regions are present in the edges of the regional model domain. In these situations, the interpolations between the GCM and RCM resolution can produce (unrealistic) extrapolations beneath the surface of the driving model. This issue is not explicitly mentioned in most of the studies, but the domains used follow the suggestions in Jones et al. (2004) to locate the areas of interest far from the edge of the domains and to avoid placing the edge of

the regional domain over mountainous regions, an instruction which has been adhered to in choosing the domains for the present study.

Item 7 is domain size, which is not a settled issue. The work of Jones et al. (1995) and Bhaskaran et al. (1996) showed different results when it came to sensitivity to the domain size. The size of domains used in the reviewed studies varied widely. Ideally a sensitivity study to determine the ideal domain along the lines of what Jones and Bhaskaran did would occur for each regional modelling experiment, but the majority of studies do not explicitly report taking such a step. In the current study, the choice of domains relied mainly on recognised experts rather than sensitivity studies due to time constraints. For the South Asia region used in this study, which was recommended by Balakrishnan Bhaskaran as a result of his own research over the same region (Bhaskaran et al. 2006, 2008), such a study already took place. For the European region, which corresponds exactly with the region used by the European ENSEMBLES project, the author suspects that the choice of domain was largely politically determined (to include all EU member states), with approval by experts already familiar with optimal domain sizes for Europe.

Item 8 (quality of the driving data) is an unavoidable issue for RCMs nested into GCMs. Because the RCMs depend on GCMs (or observational re-analysis data) for input, there is a garbage-in garbage-out expectation. The authors reviewed frequently attributed poor RCM performance to poor quality GCM driving data in that area of the world (as well as attributing high quality simulations to high quality driving data from the GCM). This issue is one of the main reasons for driving RCMs with re-analysis data, as there is much higher confidence in the quality of re-analysis data than driving data from a GCM. If the RCM performs poorly, then the likelihood of poor quality driving data is lessened, allowing for a more certainty in describing the model's performance.

The final item in Table 2.1 is climate drift or systematic error. Climate drift (in which the models establish unrealistic equilibrium climates) in GCMs is much improved, as evidenced by the number of GCMs in AR4 which ran without flux adjustments to sea surface temperatures as compared to the number of GCMs needing flux adjustments in the IPCC Third Assessment Report. Still, there is the possibility that RCMs could exhibit climate drift, though this does not seem a major likelihood for RCMs which are atmosphere-only and thus given prescribed SST values. As far as systematic error, all the of the previously mentioned items and more are possible sources of systematic error, and in this authors opinion much more work needs to be undertaken to isolate the sources of these errors, such as the work of Noguer et al. (1998), Denis et al. (2002, 2003) and Laprise (2008).

In this author's opinion, one more area of improvement pertains to the climate modelling published reports and articles. The qualitative description of model performance is often down

to the authors themselves and can be subjective. For example, what one author describes as "good agreement" might be described quite differently by another author. These qualitative descriptions are usually accompanied by (non-subjective) mathematical descriptions (e.g. correlation coefficient), but the subjective description is what is given greater emphasis in the long run as it is easier for the reader to connect with and retain, particular the non-technical reader. This is why a clearly defined meaning to descriptive words as given in AR4 (in which words such as "likely", "very likely, "virtually certain", etc. are given numerical definitions) is necessary and worthwhile. This author aspires to adhere to clearly defined descriptive language in this study.

Chapter 3

Design of Experiments and Analysis Methods

In this study, the quality of the representation of extreme precipitation as produced by HadRM3P over four different climatic regions of the Earth is assessed against historical observational data, allowing for the computation of objective measures of the skill of the model. The four regions examined are Europe, the continental United States, Southern Africa and South Asia.

Over each of the four regions, HadRM3P is driven by the ECMWF ERA-40 (Uppala et al., 2005) re-analysis data for a 42 year period spanning December 1957 to December 1999. The horizontal resolution used is 0.44° by 0.44° (50 km by 50 km). The first model year (December 1, 1957 to November 30, 1958) is considered as the model spin-up and discarded from the analyses (see section 3.3.5). The outer eight lateral grid points for all data are discarded as by-products of interpolation of the driving data to the RCM grid (See section 3.3.4)

Use of boundary data from a re-analysis keeps biases in the driving data small compared to boundary forcing from a GCM. This allows for isolation of RCM downscaling errors by comparison with observations during the period the RCM is run (Frei et al., 2003; Noguer 1998).

For the evaluation of the RCM simulations of extreme precipitation, high quality observational data sets with measurements recorded at high temporal and spatial density are essential. Such events occur infrequently and thus have a small sample size.

The observational data sets used in this study have the benefit of offering daily values of precipitation for over 40 years, sufficiently long to obtain large enough samples of extreme events as defined in this study. With the exception of the observational data set used for India, the rest of the data sets have the same or a higher resolution than the model. A

common validation period of 41 years, 1 month (December 1958 to December 1999) is used in this study as this time period represents the available time covered by the model and all four observational data sets used in the four climatic regions.

Knowledge of the climate zones of each of the regions, especially in relation to extreme precipitation spatially and temporally, is important to be able to diagnose the performance of the model.

3.1 Observational Data

Four observational data sets of daily precipitation which span the common validation period are used in analysis of HadRM3P for extreme precipitation, and the ERA-40 re-analysis 'quasi-observed' boundary data is used to drive the model at its lateral boundaries.

3.1.1 ERA-40

The ERA-40 re-analysis is the output of the ECMWF high resolution GCM when driven (where available) by guiding values of historical meteorological observations. The global meteorological observational network records observations at a single location. Where observation stations are numerous and relatively dense spatially (e.g. lowland areas in the developed world), area averaging of stations within a GCM or RCM grid box can occur in order to compare to model output data. However, when the network is much less dense, such as in less developed (e.g. much of Africa) or less hospitable parts of the world (high mountains, over the oceans, the polar regions, the upper atmosphere), it becomes problematic to assess model performance in these data sparse areas. By producing a global data set largely constrained by observational data, these gaps in historical observations are filled, providing reasonable estimates of past meteorological observations for the entire globe that describe the state of the atmosphere, land and ocean-wave conditions.

ERA-40 comes with its own uncertainties. Systematic errors in ERA-40 are identified in Jung et al. (2003, 2005), including Arctic atmospheric circulation, cloud representation and stratospheric temperatures. Bromwich and Fogt (2004) found shortcomings in ERA-40 surface and upper-air data over high latitudes of the southern hemisphere as compared with observations. The quality of ERA-40 improves considerably after 1979 and the advent of satellite based remote sensing (Hertzog et al., 2007; Graversen et al., 2007). Despite these issues, re-analysis data has been treated as quasi-observational boundary data in a number of experiments (Noguer et al., 1998; Frei et al., 1998; Frei et al., 2003; Prömmel et al., 2008;

Christensen et al., 2007, Salzmann et al., 2006) as it is for the purposes of this study.

For PRECIS purposes, ERA-40 six hourly output data were post-processed in order to produce the prognostic variables needed to drive HadRM3P. This has led to creation of a global gridded data set containing 192 points longitudinally and 145 points latitudinally (1.875° x 1.25°). This data set provided the driving data for the RCM runs in each of the four regions.

3.1.2 European observations

The observational data used are a land-points-only gridded daily precipitation accumulation from the EU funded ENSEMBLES project (Ensemble-based Predictions of Climate Change and their Impact, see Christensen et al., 2007), specifically the Research Theme 5 project (see Haylock et al., 2008). The observations cover the entire ENSEMBLES region, meaning all land points in the regional model domain (all of Europe as well as areas of the north African Mediterranean coastline). The horizontal resolution is 0.44° (50 km x 50 km) on a rotated coordinate system which is identical to the rotated coordinate system used in the model run. Over sea points observations are not present; in these points the data set contains missing data indicators.

The ENSEMBLES Research Theme 5 observational data sets (hereafter RT5) are a new product which improve on previous European daily observations in spatial resolution, geographic extent, available time period, number of stations which contribute to the data set and the method used for spatial interpolation of daily climate observations. The number of stations used is up to 2316 (with the exact number varying over time). In all areas, an interpolation method was used that allowed for uncertainty estimates to be made in the interpolation. Cover over central, western and northern Europe is dense compared to station density in western Russia and north Africa (meaning high levels of uncertainty for these and any other data sparse areas and a reduction in their utility for model validation). The interpolation methods used (spline and kriging) as well as the grid box averaging have an expected smoothing effect on the extremes represented in the point observation values. The same smoothing can be expected in regional climate models at the same spatial scale, meaning this data is suitable for comparison to RCM runs (Haylock et al., 2008).

3.1.3 Southern African observations

The observations used over Southern Africa are a gridded daily precipitation accumulation (Hewitson and Crane, 2005). The horizontal resolution of this data set is 0.25° x 0.25° on a regular latitude-longitude grid over land points only. The observations cover the nations of

South Africa, Lesotho and Swaziland, as well as southern Namibia and an area of southeast Botswana along the border with South Africa. Other areas of the regional domain are not available for comparison with this data set. Values over points not in South Africa (including ocean points) are represented by missing data indicators in the data set.

The station density of the observations is relatively uniform across South Africa apart from the arid parts of northwest South Africa and southern Namibia. A range of approximately 1800 to 3500 stations are used with the number varying in time according to availability of data and quality control considerations on the station data. A method of interpolation which Hewitson and Crane refer to as "conditional interpolation" is used to estimate daily gridded area-average precipitation from point values taken from station observations. This approach recognises that values measured at each station represent a mixture of the unique station values along with a synoptic scale forcing that is shared with neighbouring stations.

3.1.4 Continental USA observations

Observational data used come from the US Unified Daily Precipitation Analysis (hereafter UDP) data set (Higgins et al., 2000). The horizontal resolution of the data set is 0.25° x 0.25° on a regular latitude-longitude grid. This observational data set extends from 140°W to 60° W and 20° N to 60°N. The data is valid over the continental USA only, which lies between 20°N and 49.5°N and 126.25°W to 67.25°W. There are 13000 stations in use after 1992 and 8000 prior to that. Data coverage is relatively uniform, with less dense coverage over the northern Great Plains states and the desert areas in the west. The data were quality controlled to eliminate duplicates and station overlap, and buddy checks and standard deviation tests were applied. The data were then gridded onto a 0.25° by 0.25° grid using a Cressman interpolation scheme. This data set has been made use of in over 50 published studies to date.

The original UDP data set spans the period 1948-1998. Later 1999-2002 were added to the UDP, though the data sources were different for this period. The Climate Hazards Group at the University of California Santa Barbara created a Standardized Precipitation Index (Husak, 2006) using the UPD. As part of the process of creating this index a three year overlap period (1996-1998) of the original "historic" period and the later "recent" period were compared. The results showed a high correlation between data from the historical and recent data sets with small mean differences, with the conclusion that both could be used side by side.

3.1.5 South Asian observations

Observations used are the Indian Meteorological Department 1.0° gridded daily precipitation

accumulation over India (Rajeevan et al., 2005, 2006) for land points only on a regular latitude-longitude grid. Data from 1803 stations with a minimum of 90% data availability was quality controlled and then gridded to 1.0° using the Shepard interpolation method with directional effects. The stations used in forming the data set are concentrated especially in southern and western India, with data sparse areas in the north (i.e. Kashmir, Jammu and Uttar Pradesh) and the east (i.e. India east of Bangladesh).

3.1.6 Observational uncertainty

The four observational data sets utilised differ from each other in terms of horizontal resolutions, coordinate systems, geographical extent, station density, and quality control and interpolation schemes. This means that the model performance over one climatic region (in comparison to the observations used) is not directly comparable to model performance over the other regions studied. This creates a source of uncertainty in assessing the model skill.

To investigate uncertainty in the observations, the model output data for the four regions was compared to another data set of daily precipitation, the US Climate Prediction Center (CPC) Unified Gauge-Based Analysis of Global Daily Precipitation (Chen et al., 2008). This data set has global coverage over land points at 0.5° for the period 1979-2005, representing the post satellite era of observations.

The CPC data were found to have very high quality coverage over the United States, yielding results with 10% of the UDP data, but in the other three regions the results were inconclusive. In the case of India in particular, the observations showed significant dry biases in area average annual and seasonal mean precipitation, on the order of 50% (not shown). Thus the CPC observational data were excluded from the formal analysis to maintain experimental clarity, though the inclusion of more observational data sets to the validation of the model is an area of potential further work in the validation process.

3.2 Study Regions

3.2.1 Europe

Most of Europe is a temperate zone marked by year-round rainfall and a relatively small temperature range between seasons. The Gulf Stream and North Atlantic current mean that the climate of Europe is warmer on average than its high latitude might otherwise suggest. The majority of rainfall originates from low pressure systems which are driven eastward by

prevailing westerly winds.

The southern parts of Europe and the northern coast of Africa have a Mediterranean climate with hot, dry summers and cool, wet winters. These areas receive the majority of their rainfall during the October to March period. Much of Europe, including the UK and Ireland, France, Germany, Denmark, Poland, southern Iceland, southern Sweden, southern Finland and the west coast of Norway have a maritime climate. The annual temperature range is smaller than that seen in the Mediterranean climate areas, and precipitation is year-round with less incidence of heavy rainfall due to storms and more occurrence of wet days with smaller daily rainfall amounts.

Areas in the interior of the continent, excluding the Alps, are farther from the influence of the Atlantic ocean and have continental climates with a larger range of seasonal temperatures. Hot, humid summers and cold, often snowy winters are normal. The areas in northern Iceland, eastern Norway, northern Sweden and northern Finland have drier, colder climates than the other parts of these countries due to the influence of the Scandinavian mountains in weakening weather systems and their proximity to the Arctic.

The regional dimensions used for the HadRM3P RCM run over Europe correspond exactly with dimensions used by regional modelling experiments in the EU funded ENSEMBLES project (Ensemble-based Predictions of Climate Change and their Impact, see Christensen et al., 2007). This domain contains 118 grid points longitudinally and 115 grid points latitudinally, in an area north-south from 23° N to 74° N and east-west from 45° W to 62° E. The coordinates of the rotated pole are (39.25° N, 198° E). See Figures 3.1 and 3.2 for plots of the regional model domain's orography, on the rotated coordinate system (Fig 3.1) and on a regular latitude longitude coordinate grid (Fig 3.2).

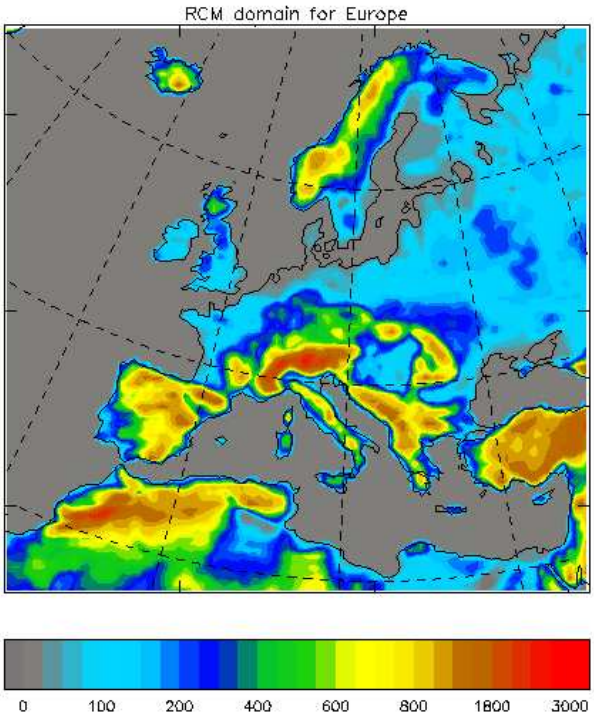

Figure 3.1: Regional model domain orography (m) for the European region on the rotated coordinate system.

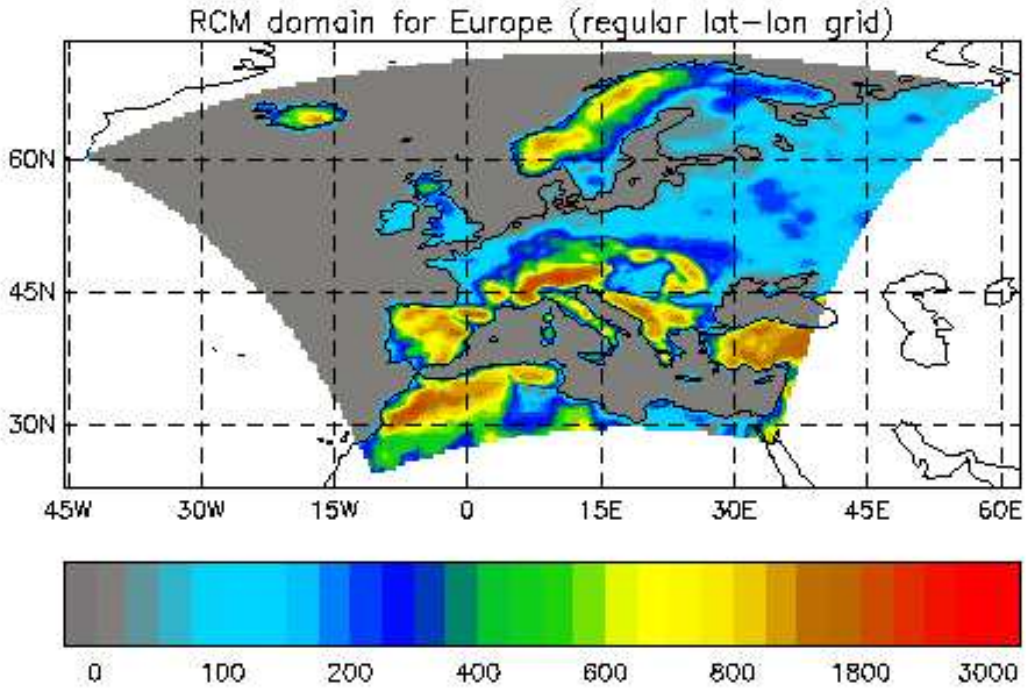

Figure 3.2: Regional model domain orography (m) for the European region on the regular latitude-longitude coordinate system.

3.2.2 Southern Africa

Southern Africa contains a wide variety of climate zones due to the influence of ocean currents, the mechanics of global atmospheric circulation and the elevation of the land areas (see Kottek et al. 2006 for an updated Köppen-Geiger Climate Classification).

South Africa itself contains several different climatic areas due to the presence of ocean on three sides and the varied topography of the country. The high plateau in the interior (the "veld" area) occupies an elevated plateau that translates into colder temperatures relative to coastal areas. Winters are dry and mild, with summer rainfall in the form of convective storms the major source of precipitation. The south-western Cape area receives most of its rainfall in winter and is characterised by a Mediterranean climate with mild winters and warm to hot dry summers with occasional rainfall and changeable weather in general. Temperatures along the west coast (influenced by the Benguela current) can be in sharp contrast to areas on the east coast that are warmed by the Agulhas current. The eastern part of the country in general is wetter than the western part due to influence from trade winds coming off the Indian Ocean. Summers in the east are warm and rainfall occurs year-round.

Desert areas occupy southwest and western Namibia, southwest Angola, southwest Botswana and northwest South Africa due to descent of dry air from the Hadley cell meeting with the cold Benguela ocean current that originates in Antarctica. These areas receive less than 10mm of annual rainfall on average. These areas are generally very hot, apart from the west coast of Namibia which is cooled by the Benguela current.

The regional dimensions used for the regional model run over Europe are identical to the dimensions of the regional model run carried out by Hudson and Jones (2002b). The region contains 113 grid points longitudinally and 102 grid points latitudinally, in an area north-south from 41° S to 1° S and east-west from 2° E to 56° E. The coordinates of the rotated pole are (67.5° N, 30° E). See Figure 3.3 for a plot of the regional model domain's orography on the rotated coordinate system.

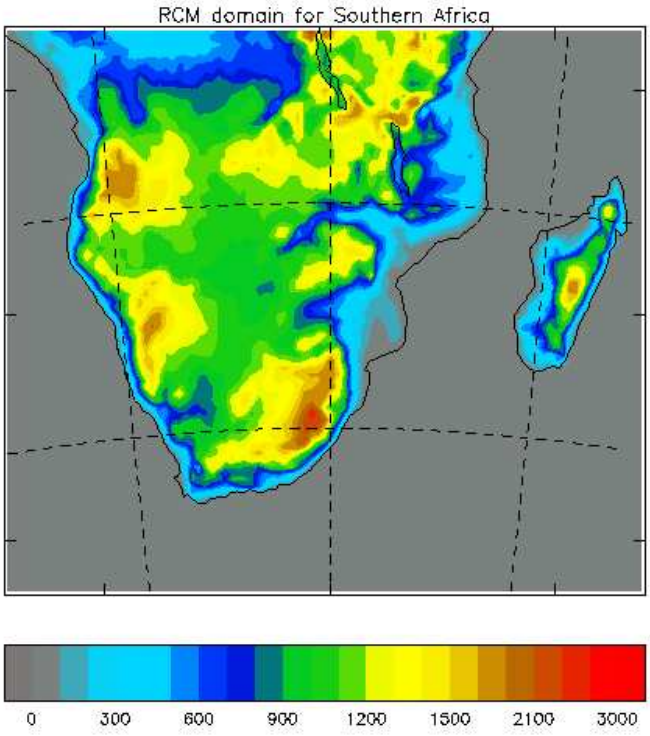

Figure 3.3: Regional model domain orography (m) for the Southern African region on the rotated coordinate system.

3.2.3 Continental USA

The climate of the continental United States is strongly influenced by the position of the polar jet stream, as well as land-surface features (plains, mountains) and geographical location. The country lies in an area of westerly air movement and as such can feature large frontal systems.

The eastern half of the country (roughly meaning east of the Mississippi river) is a temperate climate. The climate is generally humid with four well defined seasons and year round rainfall. The southeast is a subtropical area with hot, humid summers and milder winters. Southern Florida is the exception, as its position further south and influence of the ocean on three sides give it a tropical savannah climate. These coastal areas of the southeast are most vulnerable to tropical cyclones and requisite extreme precipitation during the hurricane season of June to November. The northeast features more continental weather. Summers are warm to hot, while winters can be cold and snowy. In winter, the polar jet stream can combine with other pressures systems and cause snowstorms and blizzards.

The Great Plains areas are situated between the Rocky Mountains and the areas west of the Mississippi. This area is characterised by flat, grassland terrain and a continental, semi-arid climate with hot summers and cold, dry winters, with large extremes in temperature. When the polar jet stream brings in low pressure systems from the Pacific to these areas, the flat terrain can allow for the systems to reorganise and clash with other air systems, causing strong thunderstorm activity and tornadoes. Rainfall can thus be unpredictable, meaning these areas are vulnerable to droughts and localised flooding.

The Rocky Mountains area stretches from New Mexico in the southwestern United States to the Canadian province of British Columbia in the Pacific Northwest. This area features a highland climate in which elevation has the biggest impact on local climate. Generally, summers are mild and dry, while winters can be extremely cold and very snowy. Weather can change very quickly due to the mountains' effects on the wind. This area receives sufficient precipitation to be heavily forested.

The southwestern United States (Arizona, western New Mexico, Utah and Nevada, south-eastern California) are desert areas with dry, warm weather year-round. The majority of precipitation that these areas receive occurs during the North American monsoon period from late May to July. Brief but powerful rainstorms can occur during this time that can cause flash floods. El Niño and La Niña have an established teleconnection with winter weather in the southwest, with El Niño meaning wetter winters and La Niña dry winters in comparison to average winter weather.

The west coast areas feature Mediterranean (California) to maritime (Pacific Northwest) cli-

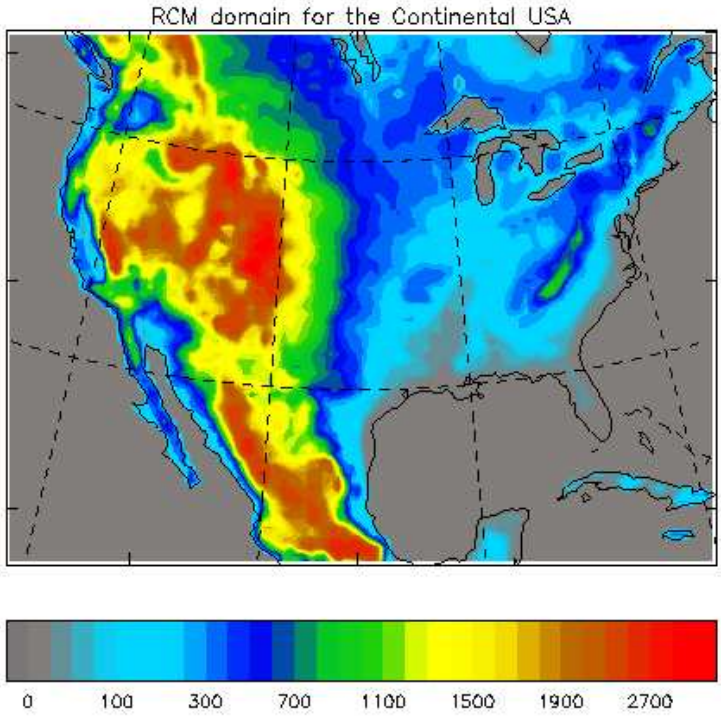

Figure 3.4: Regional model domain orography (m) for the continental United States region on the rotated coordinate system.

mates with warm, dry summers and wet winters. The temperature range year-round is relatively narrow in comparison to the other climate areas in the region. Moist air masses originating in the Pacific are the major source of winter precipitation.

Figure 3.4 shows the orographic height for the domain used in the simulation over the continental USA. The domain contains 122 grid points longitudinally and 96 grid points latitudinally, in an area north-south from 16° N to 53° N and east-west from 133° W to 62° W. The coordinates of the rotated pole are (52.83° N, 81.59° E).

The domain contains the whole of continental USA as well as northern Mexico, Cuba, Jamaica, and southern Canada along the US border. The domain was chosen to be sufficient to capture the large-scale westerly flow which results in the majority of precipitation for the USA, as well as resolving the entirety of the Gulf of Mexico, which is an area of cyclone activity that can experience extreme precipitation due to hurricanes and tropical storms.

3.2.4 South Asia

The climate of South Asia is very diverse thanks to the Himalayas to the north, the Indian Ocean to the south, the western Ghats along the west coast of India, and the southwest summer monsoon. In the majority of areas there are four seasons: winter (December, January and February), summer (March to May), a rainy monsoon season (June to September) and a post monsoon period (October and November). Areas in the north of the region (south of the Himalayas) also have a spring and autumn period.

The southwest summer monsoon has the largest influence on climate and especially precipitation in that the vast majority of rainfall received in south Asia is during the monsoon season. During this period, a reversal to the prevailing circulation occurs due to a northward shift to the jet stream. Warm, moist air from the Indian Ocean to the southwest is ferried north-eastward. The Intertropical Convergence Zone (ITCZ) which is normally located near the equator, also experiences a northern shift. The onset of the monsoon varies according to geographical location, starting at the end of May in the south and moving north-west to start in late June in the north. By July most of South Asia is experiencing heavy rainfall. The southwest summer monsoon weakens during September and is gone by early October.

Regionally there are variations in climate due to topographic influences. The areas in the north of the region have the high mountains of the Himalayas and the Hindu Kush as well as the Tibetan plateau. Due to the sharp gradients in elevation and accompanying decrease in temperature due to altitude, large differences in climate can exist in areas only tens of kilometres away. The mountains and plateau areas can be extremely cold and snowy during the winter months, with rainfall occurring during the warmer May to September period.

The areas just south of the Himalayas have an alpine climate type. The mountains act as natural barriers to cold continental winds originating in central Asia. On the northward slopes of the Himalayas the moisture in these winds is rained or snowed out, leaving the downhill winds drier. Thus areas immediately south of the mountains are mild during winter and hot during the summer. These areas are exposed to the southwest monsoon and thus receive the majority of their rainfall during this season.

Several large areas are arid or semi-arid regions, including the northwest areas of India, central and northern Pakistan, and areas in south central of India east of the Western Ghats. Rainfall these areas receive is left over from the monsoon, which can be late or fail to appear altogether.

The southwest coast of India (west of the Western Ghats) is a tropical wet climate, with persistently warm or hot temperatures year-round with large amounts of rainfall during the monsoon period. A drier, tropical wet and dry climate characterises most of inland India. Winters are long and dry, while summers can be exceptionally hot. The monsoon brings heavy rain from June to September. Some areas of southern India can experience winter rainfall via a northeast monsoon beginning in late September which carries dry air (moistened by the Bay of Bengal) from the northeast towards the southwest.

Bangladesh, northeast India and much of North India experience hot summers and cold temperatures during the winter months. This region features very little winter precipitation during the winter due to downhill (katabatic) dry winds flowing south from the Himalayas and Central Asia. The majority of rainfall occurs as thunderstorm associated with the southwest monsoon during the rainy season.

Extreme precipitation in the form of torrential rains can occur during the monsoon season in much of South Asia. Additionally, coastal areas are subject to tropical cyclones which are generated in the warm waters of the Indian ocean north of the ITCZ and in the Bay of Bengal due to intense summer heating. The tropical cyclone season lasts from April to December, peaking May to November. Most cyclones occur in the Bay of Bengal, making landfall along the eastern coasts of India, southern Bangladesh and western Burma, although cyclones can also occur in the calmer Arabian sea as well.

The regional dimensions used for the regional model run over South Asia were suggested by Balakrishnan Bhaskaran (personal communication) based on his own regional modelling work over the same area. The domain used is the same as "RCM3" in Bhaskaran et al., (1996), with the exception that the western boundary is 5 degrees further west in "RCM3." The region contains 80 grid points longitudinally and 80 grid points latitudinally, in an area north-south from 2° N to 37° N and east-west from 63° E to 103° E. The coordinates of the rotated pole are (75.27° N, 257.33° E). The region contains the whole of India, Sri Lanka, Bangladesh, Nepal and Bhutan as well as most of Pakistan and western Burma. See Figure 3.5 for a plot of the regional model domain's orography on the rotated coordinate system.

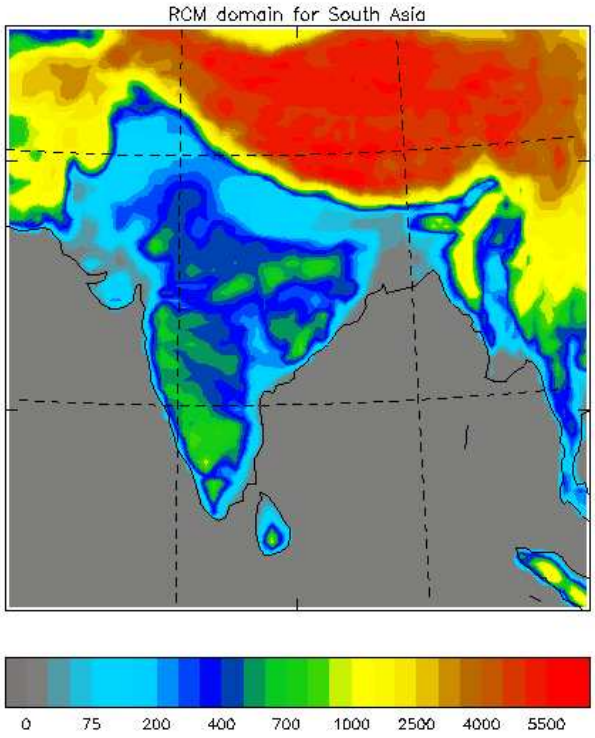

Figure 3.5: Regional model domain orography (m) for the South Asia region on the rotated coordinate system.

3.3 HadRM3P description

At the core of PRECIS is the HadRM3P (Hadley Centre Regional Model version 3, PRECIS Physics), regional model, ported to run on a PC.

The HadRM3P model is based on the HadAM3H high resolution GCM (Hudson and Jones, 2002a), which is an improved version of the atmospheric component of the HadCM3 (Hadley Centre Coupled Model version 3) atmosphere and ocean GCM (Gordon et al., 2000) with substantial modifications to the model physics. HadRM3P uses the same formulation of the climate system as is used in HadAM3H. The grid scale dynamics and sub grid scale physics are largely identical in the RCM and GCM with account taken for those elements which are resolution dependent. This is important to help ensure that the RCM provides high resolution regional climate change projections generally consistent with the climate change projections of the parent GCM.

HadRM3P is a hydrostatic atmospheric and land surface model of limited area and high resolution which is locatable over any part of the globe. Dynamical flow, clouds and precipitation, the atmospheric sulphur cycle, radiative processes, the land surface and the deep soil are all described. The model diagnoses these processes as it evolves in time.

3.3.1 Dynamics and Horizontal and Vertical Grid

Dynamical flow and thermodynamics are modelled throughout the atmosphere. Special consideration is given to the model formulation in the boundary layer and account taken of the modifying effects of mountains. The model dynamics are associated with the advection of the meteorological state variables present in the lateral boundary conditions. The atmospheric component of HadRM3P is a hydrostatic version of the primitive equations used to approximate atmospheric flow. The primitive equations consistent of differential equations utilising five variables (zonal velocity, meridional velocity, vertical velocity, temperature and geopotential) as well as the Coriolis force to represent conservations of mass, momentum and energy for dynamical flow on the surface of a sphere. The atmosphere is assumed to be in a state of hydrostatic equilibrium. As such vertical motion is diagnosed separately from the diagnosis of the primitive equations. The model has a complete representation of the Coriolis force.

HadRM3P has been designed to run with horizontal resolutions of 50 or 25 kilometres on a regular latitude-longitude grid, and the atmosphere is represented by a hybrid sigma vertical coordinate system (Simmons and Burridge, 1981). Vertically there are 19 model levels, the lower four levels purely terrain following sigma coordinates, the upper three levels on pressure levels only, and the middle levels a mix of the two. The bottom atmospheric level is located

between the surface and approximately 50 metres and the highest vertical level is located at 4.6 hectopascals.

The latitude-longitude horizontal grid of the regional model is rotated so that the equator lies within the region domain. This is done in order to obtain as close to uniform grid box sizes as possible throughout the region as well as to remove the need for filtering at high latitudes. In GCMs, Fourier filtering must take place due to much smaller areas of grid boxes in locations greater than 60 degrees north and less than 60 degrees south. In these areas the meridians begin to converge towards the poles. The primitive equations are solved in spherical polar coordinates. The exact horizontal resolution is 0.44 by 0.44 degrees (0.22 by 0.22 degrees), which provides for a 50km (25km) resolution at the equator of the rotated grid, requiring a dynamical timestep of 5 minutes (2.5 minutes) to maintain numerical stability at these resolutions. An Arakawa B grid (Arakawa and Lamb, 1977) is used for horizontal discretization to improve the accuracy of the split-explicit finite difference scheme. In this horizontal layout, the momentum (wind) components are offset for half a grid box in the east-west and north-south directions from the other thermodynamic variables (surface pressure, temperature and humidity) and aerosol variables.

Horizontal diffusion is applied to the wind, temperature, and humidity variables in order to provide representation for unresolved sub grid scale processes as well as to control accumulation of grid scale noise and energy. Fourth order diffusion is used throughout, except on the top level for the winds and temperature, where second order diffusion is applied to prevent excessive stratospheric jet speeds at the top of the atmosphere. The order of diffusion and diffusion coefficients are dependent on the model resolution utilised.

Geostrophic adjustment is separate from the part of the model's integration which deals with advection. This adjustment is iterated three times per 5 minute advection timestep. The three adjustment timestep are then averaged to obtain the velocities used for advection, which is integrated in time using the Heun scheme (Mesinger, 1981). This finite difference scheme is 4^{th} order accurate except at high wind speeds when it is lowered to 2^{nd} order accuracy for stability purposes. The numerical form of the dynamical equations formally conserves mass, momentum, angular momentum and total water in the absence of source and sink terms.

3.3.2 Physical Parameterisations

Components of the climate system which operate below the grid box scale of the GCM but which exert important influences on the climate as a whole must be parameterised. Example of these quantities include the representation of clouds, convection and convective precipitation, surface exchanges, and boundary layer related issues. Parameterisation is a grid box area

estimate of the effect of a sub grid scale component responding to the larger grid scale state of the system.

Parameterisations that relate to extreme precipitation are relevant to this study as these model physics exert an influence on modelled rainfall. A mass flux penetrative convection scheme (Gregory and Rowntree, 1990) is used with an explicit downdraught (Gregory and Allen, 1991). It includes the direct impact on momentum, heat and moisture of vertical convection (Gregory et al., 1997). Convective precipitation does not change phase if the latent cooling would take the temperature below freezing again. Evaporation or melting of convective precipitation is accounted for.

Large scale clouds and convective clouds are dealt with separately in how they are formed, their precipitation and radiative effects. Cloud water content (liquid and frozen) and layer cloud cover in a grid box are both calculated from a saturation variable that is defined as the difference between total water and the saturation vapour pressure. Values of the grid box mean relative humidity are calculated at each timestep and are used in determining the fraction of cloud cover in a grid box. Cloud water is assumed to be frozen below -9° C, liquid above 0° C, and a mixture of the two in between. Layer cloud can form at any vertical level apart from the top of the stratosphere (the top level of the model). Large scale precipitation from layer cloud depends on cloud water content. Evaporation of large scale precipitation is accounted for as are enhanced precipitation rates via seeding from layers above. Large scale precipitation is assumed to fall on 75% of land surface, regardless of layer cloud fraction.

Sulphate aerosols are accounted for in the representation of the effective radius of cloud droplets, which is modelled as a function of cloud water content and concentration of the number of droplets (Martin et al., 1994). The first direct effect (scattering of and absorption of incoming solar energy) and first indirect effect (increased aerosol concentrations can produce higher concentration of droplets and increase cloud albedo) of aerosols are represented, although the second indirect effect (aerosol effect on lifetime of clouds) is not represented.

The land surface has a vegetated canopy which interacts with the flow, incoming radiation and precipitation and provides heat and moisture fluxes. The land surface scheme employed is MOSES (Met Office Surface Exchange Scheme, Cox et al., 1999). Soil hydrology and thermodynamics are represented using 4 layers for temperature and moisture.

Full details of all physical parameterisations are provided in Jones et al. (2004) and Buonomo et al. (2007)

3.3.3 The Atmospheric Sulphur Cycle

HadRM3P also contains a representation of the atmospheric sulphur cycle, accounting for sulphur dioxide, sulphate aerosols and dimethyl sulphide. These modes represent sulphate particles dissolved in cloud droplets plus two free particle modes (the Aitken mode and accumulation mode). The model simulates the transport of these aerosol variables by horizontal and vertical advection, convection and turbulent mixing. When available, aerosol data is accounted for by six-hourly prognostic data provided at the lateral boundaries. When driven by GCMs or re-analyses which lack aerosol prognostic data, the sulphur cycle is forced internally by aerosols values taken from local emissions sources. In this configuration, the advected-in values are set to zero. They are then are prescribed local values in the regional domain which are advected inside the domain and eventually out of the domain.

3.3.4 Boundary conditions

Boundary conditions are required at the limits of the regional domain to provide the necessary meteorological inputs for the RCM to be able to run. Surface boundary conditions (time series information of sea surface temperatures and sea ice extents) are required over water points only. There is no prescribed constraint of the upper boundary of the model (except for the input of solar radiation). Lateral boundary conditions are required for the longitudinal and latitudinal edges of the regional domain. These are comprised of pressure, horizontal wind components, temperature and humidity. The specific prognostic variables are surface pressure, zonal and meridional component of wind flow, potential temperature adjusted for the latent heat present in cloud water and ice, and water vapour plus liquid and frozen cloud water (Jones et al., 1995). Lateral boundary conditions are updated every six hours, while sea surface boundary data components update once per model day.

The process of coupling the coarse resolution prognostic data to the fine scale regional resolution occurs across a linearly-weighted four grid point buffer area surrounding the regional model domain. In these four grid points, the prognostic variables are relaxed towards values interpolated in time from six-hourly data from a GCM or re-analysis. These four points utilise the orography of the GCM (shaded yellow in Figure 3.6, a sample RCM domain over the UK at 50km resolution), as well as a further four points inside the buffer area (shaded blue in Figure 3.6). This eight grid point area contains data that is biased and is therefore spurious in relation to the RCM. Because of this, data from this area must be discarded prior to any analysis. In Figure 3.6, the area suitable for statistical analysis are the grey grid points inside the red line.

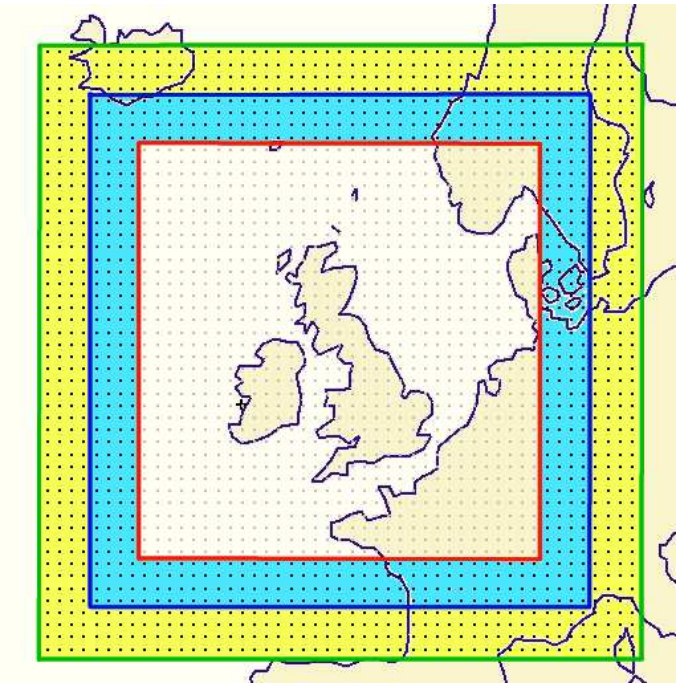

Figure 3.6: Example of an RCM domain using a 50 km grid point resolution. Areas shaded in yellow and blue are areas of relaxation between the GCM and the RCM and must be discarded before analysis is undertaken.

3.3.5 Initial Conditions and Spin-up

The regional model's starting point requires an initial state of the climate system as input. These initial conditions are formed from the driving data (GCM or observational re-analyses). The influence of the atmospheric component of the initial conditions of the model will not be retained beyond a few model days. Because the initial state is quickly forgotten, the climate problem is a essentially a boundary value problem instead of an initial conditions problem. However, the initial state of the soil variables in the land surface component of the regional model may take one to two model years before coming into an equilibrium state with the atmospheric forcings from the GCM experiment. During this 1-2 year model "spin-up" period certain variables can be biased. HadRM3P requires on the order of one model year for spin-up. This period of the simulation is unreliable due to the lack of equilibrium state. As such, model output data in this spin-up year should be discarded prior to analysis of the model's output data (and has been for the purposes of this study).

Chapter 4

Results and Analysis

Daily mean precipitation data for the model and the observations for common period (December 1, 1958 to December 31, 1999) were established via HadRM3P model runs and post-processing of observational data sets where necessary (e.g. application of land-sea mask, changing of measurement units). The model output data were converted from the SI unit of mm sec^{-1} to mm day^{-1} as this value corresponds to the unit used in the observational data sets. The observational data sets for Southern Africa, continental USA and Europe (all at the same or a finer resolution than model output data) were regridded (via data aggregation) to the 0.44° rotated coordinate system of the model. In the case of South Asia, the observational data set was at a coarser resolution (1.0°) than the model output, so for this region the model output was aggregated to a 1.0° resolution.

4.1 Wet day threshold

Numerical noise and truncation errors in climate models can produce very small values of precipitation. As such, it is useful to define a **wet day** as being a day in which the daily rainfall accumulation exceeds a set threshold amount. In this study, a threshold value of 0.1 mm day^{-1} is used for all statistical analysis over Europe, the continental USA and Southern Africa. Over India a threshold value of 1.0mm day^{-1} is used. These value has been chosen for several reasons. During testing to determine optimal threshold amount, it was found that setting the threshold amount to a higher value (e.g. 1.0 mm day^{-1}) in climatically dryer areas caused the mean values in the upper tail of the distribution to be higher, as there were a significant number of rainfall events between 0.1 mm day^{-1} and 1.0 mm day^{-1} which were excluded by use of the higher threshold value. Along with this, the higher threshold value lowered the per-grid point sample size (i.e. the number of grid points used to calculate the

upper tail) such that in drier areas, sample sizes were insufficiently large enough for confidence in results. A threshold value of 0.1 mm day^{-1} has had widespread use in research involving models and precipitation (e.g. Kendon et al., (2008); Semenov and Bengtsson (2002); Solman et al. (2008)). For South Asia, a higher threshold value of 1.0 mm day^{-1} is utilised due to the lower density of rain guages per grid point in the observational data sets coupled with the coarser resolution, as the two in concert can lead to underestimation of light area-averaged precipitation events.

4.2 Indices

Four indices are examined in analysis: seasonal mean, wet day intensity, wet day frequency and extreme precipitation.

Seasonal mean precipitation was calculated for model output data and observations for each of the four regions. The multiannual seasonal mean provides a "big picture" view of the model's performance in comparison to observations, as it takes into account each grid point value over the full common period. Seasons were defined as December-January-February (DJF), March-April-May (MAM), June-July-August (JJA), and September-October-November (SON) for Southern Africa, continental USA and Europe. South Asia's seasons were defined as DJF, MAM, June-July-August-September (JJAS), and October-November (ON) owing to the southwest summer monsoon. The value of each grid point in the multiannual seasonal mean is the average of the precipitation value for that grid point in each day of the respective season during the 41 year common period. For example, the total number of days in 41 years worth of MAM can be determined by adding up the number of calendar days in March, April and May and multiplying them by 41 (i.e. (31+30+31)*41 = 3772).

Wet day intensity is defined as the multiannual seasonal mean of grid points containing precipitation values which exceed the wet day threshold. Wet day intensity provides information on how well the model is performing (only) when it is producing precipitation exceeding the wet day threshold. Wet day intensity allows for contrast of the amount of precipitation produced by the model to that found in observations, as this may differ considerably in comparison to a full multiannual seasonal mean which takes into account both wet days and dry days.

Wet day frequency is a fractional value that indicates the percentage of days in which a particular grid point receives precipitation exceeding the wet day threshold. A wet-day frequency of 0.25 (i.e. 25%) means that a particular grid point receives precipitation exceeding the wet day threshold on one out of every four days during a fixed length of time (e.g. 41 years). Wet day frequency provides information on how often the model produced precipitation

for a given location in comparison to how often the grid point received precipitation in the observations.

As in Kendon et al. (2008), the **extreme precipitation** index is defined as the mean daily precipitation exceeding the 95th percentile of the distribution of wet days by season. A percentile approach has been chosen in preference to other metrics such as the exceedance of a fixed threshold (e.g. Bader and Bantle (2004) defined extreme precipitation as events exceeding 70 mm in 48 hours) because use of percentiles offers better comparability between climatologically different regions and/or seasons. Percentile definitions of extreme precipitation have a history of use in past research (Roy et al. (2004); Christensen and Christensen (2003); Supiah and Hennesy (1998)).

For a period of 3772 days (e.g. MAM over 41 years), a wet day frequency of 0.50 will provide 1886 events in the full distribution for a given grid point. In that example, there will be 94 events in the upper 5% which are averaged for creating the extreme precipitation index. In areas which are drier climatologically (e.g. a wet day frequency of 0.10) the number of events in the upper 5% is reduced, in this case to 19 events. A sample which contains only a few events is not appropriate for producing an extreme index. As such, a cutoff value of 20 events is prescribed in producing the extreme precipitation index. Grid points for which the upper 5% of wet days exceeding the wet day threshold have fewer than 20 events are not taken into consideration when producing the extreme index.

One way of addressing the sample size as well as reducing grid box noise is the use of **spatial pooling** when calculating the extreme precipitation index (Semmler and Jacob, 2004). Spatial pooling considers values from neighbouring grid points as sampling from the same precipitation population due to being close together and thus to have similar precipitation intensity distributions. Spatial pooling is a way of addressing model inability to resolve phenomena with an extension of one single grid point. By pooling the data it is possible to obtain a less noisy extreme precipitation estimate. This comes at the cost of loss of some regional detail in areas in which highly localised properties affect rainfall, such as mountainous regions. Use of 3x3 spatial pooling in Semmler and Jacob (2004) as well as Kendon et al. (2008) demonstrated improvement in signal to noise ratio calculation when determining changes in future extreme precipitation due to climate change.

In this study, 3x3 spatial pooling has been used to calculate a **pooled extreme precipitation** index. Calculation of the mean of the upper 5% of the distribution of grid point values took into account the time series of wet day values for that grid point as well as the time series of values for the grid points immediately surrounding that grid point. Thus a total of nine timeseries over the wet days was taken into consideration per grid point, increasing the sample size in the tail of the distribution to nine times its (non-pooled) size. As with the

non-pooled extreme precipitation, a cutoff value of a sample size of less than 20 events in the tail is utilised.

4.3 Results

Area averaging has been carried out on all indices described in section 4.2. Area averaging produces a single numerical value as a representation of a two dimensional field by averaging all non missing data points in the field. This enables straightforward representation of model performance in table format, but comes at the cost of smoothing the varying spatial distribution of precipitation into a single value. The larger the area that is spatially area averaged, the larger this smoothing effect will be. It is thus vital to present information about spatial correlation of data sets as well as two dimensional plots to have a sufficient representation of model performance.

In the first of two tables provided in sections 4.3.1 to 4.3.4, the **Seasonal Mean, Wet Day Intensity (Wet Day Int) and Wet Day Frequency (Wet Day Freq)** indices are described in four columns. For seasonal mean and wet day intensity, Column 2 (**Mn Obs**) of the table is the area average precipitation of the observations (in mm day^{-1}). Column 1 (**Bias**) is the model bias, which is the difference of the area average precipitation of the model (in mm day^{-1}) and the observations. Column 3 (**Bias %**) is the percentage difference between the model and the observations, effectively the percentage of how much wetter or drier the model is in comparison to the observations. For wet day frequency, column 2 is the area average of the percentage values of wet day frequency for all observational grid points. Column 1 is the model bias for wet day frequency and column 3 the percentage difference of the model bias of what percentage too little or too often that precipitation occurs. For all indices, Column 4 (**Patt Corr**)is the pattern correlation between the model and the observations, which is an area-weighted spatial correlation between the two fields. Pattern correlation provides a comparison of the spatial distributions of the model and observations.

In the second table provided in sections 4.3.1 to 4.3.4, the **Extreme Precipitation** and **Pooled Extreme Precipitation** indices are described in four columns. Column 2 (**Mn Obs**) of the table is the area average extreme precipitation of the observations (in mm day^{-1}). Column 1 (**Bias**) is the model bias, which is the difference of the area average extreme precipitation of the model (in mm day^{-1}) and the observations, and Column 3 (**Bias %**) is the percentage difference between the model and observational extreme precipitation. Column 4 (**Patt Corr**) is the pattern correlation between the model and the observations.

For the purpose of analysis, **Good** is defined as a pattern correlation of 0.70 or higher and

Descriptive Term	Numerical Value
Good	Pattern Correlation 0.70 or more
	Model bias within 20% of observations
Fair	Pattern Correlation 0.50 to 0.70
	Model bias of 20% to 40% more than or less than observations
Poor	Pattern Correlation less than 0.50
	Model bias of 40% more or less than observations

Table 4.1: Descriptive terms and corresponding numerical values used in analysis

a model bias within a range of plus or minus 20%. Fair is defined as a pattern correlation of 0.50 to 0.69 and model bias in the range of 20% to 40% or -20% to -40%. Values outside of these amounts (i.e. pattern correlation of less than 0.5 and bias greater than 40% or less than 40%) are described as **Poor**. These values have been chosen based on past research studies as well as consultation with recognised experts in climate modelling as to appropriate descriptive identifiers. See Table 4.1 for a table providing these values.

4.3.1 Europe

EUR	Seasonal Mean				Wet Day Int				Wet Day Freq			
Seas	Bias	Mn Obs	Bias %	Patt Corr	Bias	Mn Obs	Bias %	Patt Corr	Bias	Mn Obs	Bias %	Patt Corr
DJF	0.21	1.7	12	0.63	-.82	4.0	-20	0.62	0.15	0.43	35	0.84
MAM	0.45	1.4	32	0.66	-.72	3.9	-18	0.50	0.19	0.35	53	0.81
JJA	0.04	1.6	2.5	0.78	-1.6	4.7	-34	0.40	0.14	0.34	42	0.81
SON	-.01	1.8	-.75	0.69	-1.4	4.8	-30	0.56	0.12	0.38	31	0.88

Table 4.2: Comparison with model output and Ensembles RT5 observational data over Europe for the common period. Values of seasonal mean and wet day intensity are in mm day^{-1}. Values of wet day frequency are unitless.

The first item of note in Table 4.2 is the how well the model is doing for DJF, JJA and SON Seasonal Means. The range of model biases are all within the **Good** classification, and their spatial correlation is **Fair** to **Good**. A plot of JJA can be seen in Figure 4.1, in which the spatial patterns of precipitation correspond well by eye in the model and observations. The same similarity is not present in MAM (Figure 4.2). Figure 4.2 demonstrates a common issue in many regional climate models in that rainfall often appears overestimated in mountainous areas, as here over the Alps and other mountains. As in mountainous areas the density of observing stations is often lower (due to inhospitable terrain) and undercatch of precipitation

EUR	Extreme (Non-Pooled)				Extreme (3x3 Pooled)			
Seas	Bias	Mn Obs	Bias %	Patt Corr	Bias	Mn Obs	Bias %	Patt Corr
DJF	2.7	15	17	0.73	3.8	16	24	0.83
MAM	3.2	16	21	0.62	3.9	17	24	0.75
JJA	0.88	20	4.3	0.33	-0.71	21	-3.3	0.36
SON	1.9	18	11	0.77	2.4	21	11	0.81

Table 4.3: Comparison with model output and Ensembles RT5 observational data over Europe for the extreme index (with and without spatial pooling). Values in mm day^{-1}.

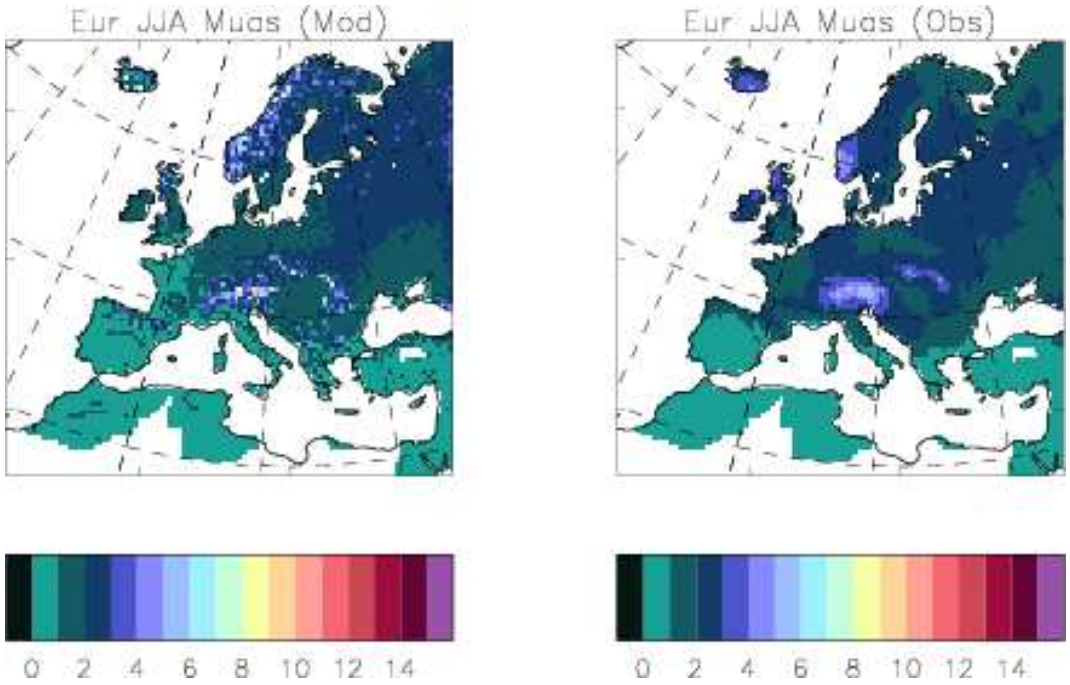

Figure 4.1: Seasonal Mean precipitation (mm day^{-1}) for Europe, JJA, model (left) and observations (right)

by gauges can be a significant problem when it falls as snow (Frei and Schar, 1998), the apparent bias could be lower than suggested. Thus the uncertainty in high altitude areas is higher than in lower altitude regions.

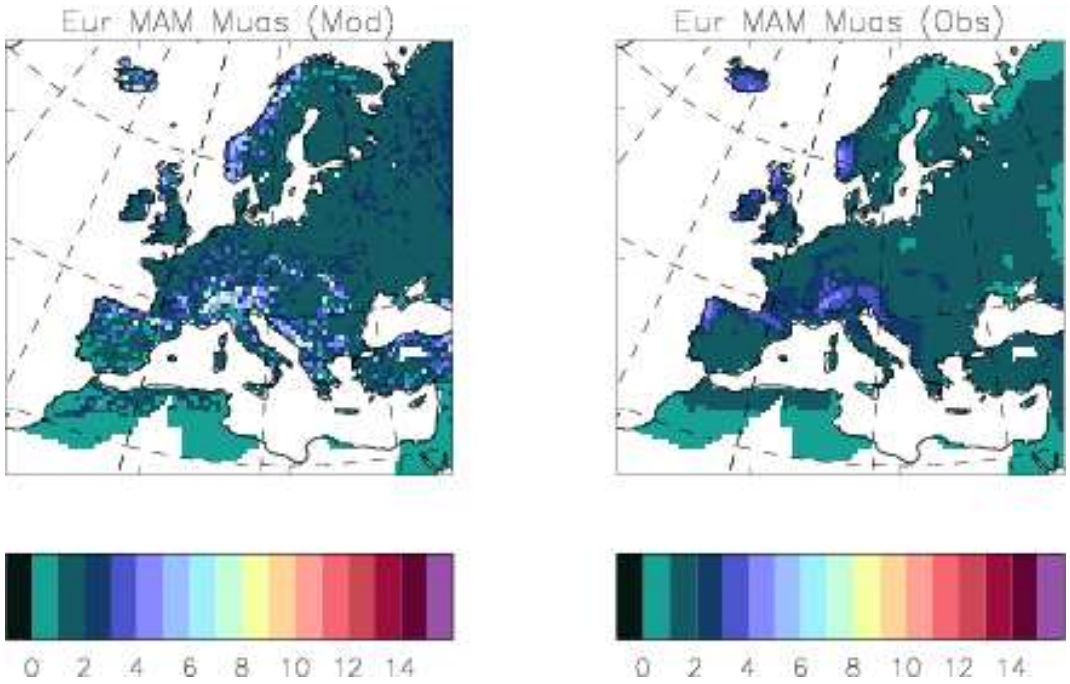

Figure 4.2: Seasonal Mean precipitation (mm day^{-1}) for Europe, MAM, model (left) and observations (right)

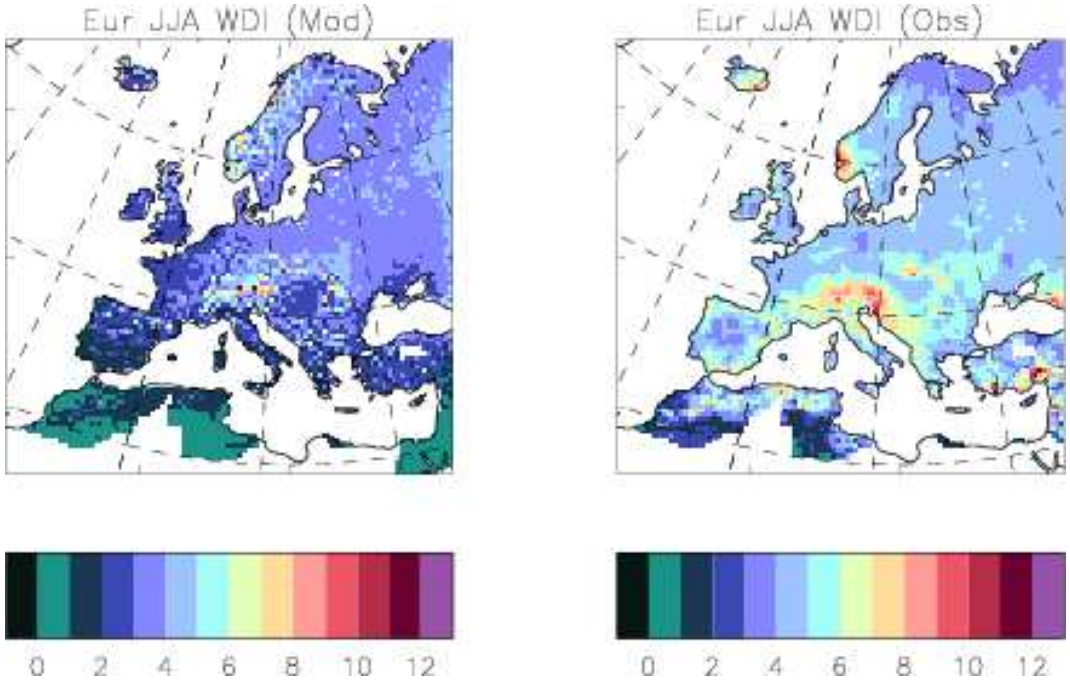

Figure 4.3: Wet day intensity (mm day^{-1}) for Europe, JJA, model (left) and observations (right)

Looking at the **Wet Day Intensity** (i.e. multiannual seasonal means of wet days) section in Table 4.2 shows the model to have a dry bias across all seasons with **Fair** performance for most indices. **Poor** pattern correlation is present in JJA. A plot of JJA can be seen in Figure 4.3 that demonstrates the model underproducing precipitation in almost the entire domain. Review of **Wet Day Frequency** shows **Good** spatial correlation for all seasons, but reveals a model that that is producing rainfall exceeding the wet day threshold amount far more often (putting it in the **Fair** to **Poor** categories) than occurs in the observations. Figure 4.4 shows that the spatial patterns where rainfall occurs in the model and observations match relatively well by eye, but that it is raining more often in the model.

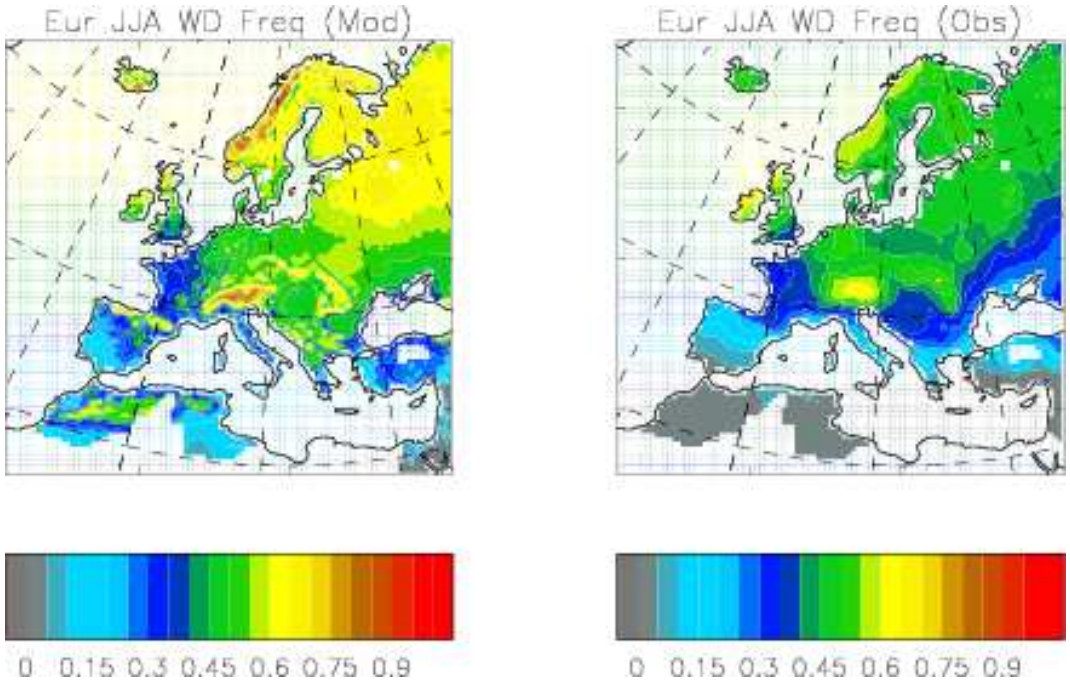

Figure 4.4: Wet day frequency for Europe, JJA, model (left) and observations (right)

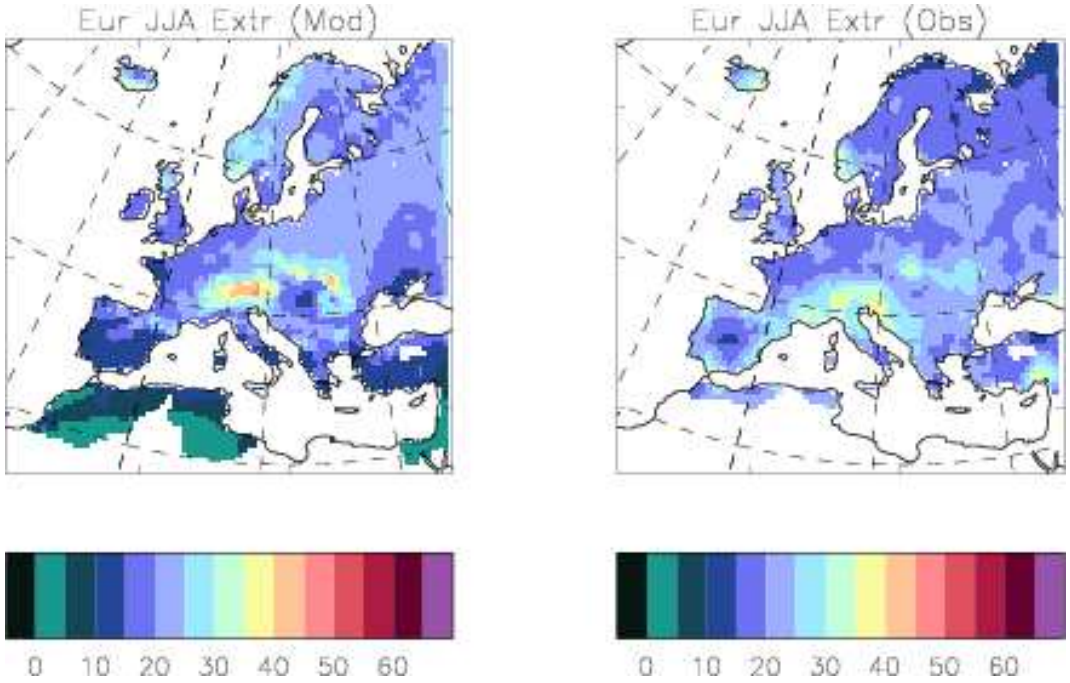

Figure 4.5: Pooled extreme precipitation (mm day^{-1}) for Europe, JJA, model (left) and observations (right)

Overall, the model appears to be producing **too many** precipitation events, but when these events occur they are **too light** in intensity. In other words, it **rains too often** in the model over Europe, **but not enough** when it does rain. One caveat to this result is that if the density of stations in the observed dataset is low then it may underrepresent low intensity events. Some evidence for this is presented in the section on South Asia.

The Extreme indices are present in Table 4.3. First of all, the spatial pooling process can be seen to have increased the pattern correlation between the observational data sets and the model in all cases. This comes at the cost of some increases to the model bias. Nevertheless, in looking at the Spatially Pooled Extreme index the model is in the **Good** category for DJF, MAM and SON for pattern correlation and bias. Performance during JJA for 3x3 pooled extreme shows a very low model bias, but poor pattern correlation (see Figure 4.5) indicating the good area average performance results from compensating regional errors. These may be due to the higher amount convective activity during this season in comparison to the other seasons. Figure 4.6 shows DJF 3x3 pooled extreme with better pattern correlation, but overpredicting extreme events in mountainous areas.

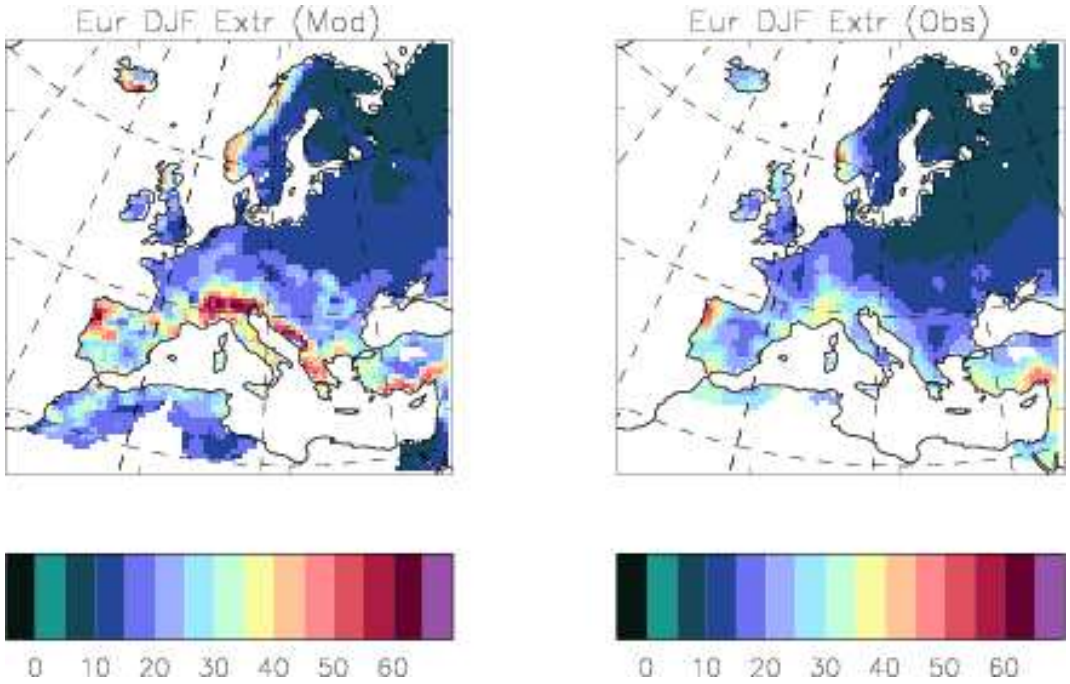

Figure 4.6: Pooled extreme precipitation (mm day^{-1}) for Europe, DJF, model (left) and observations (right)

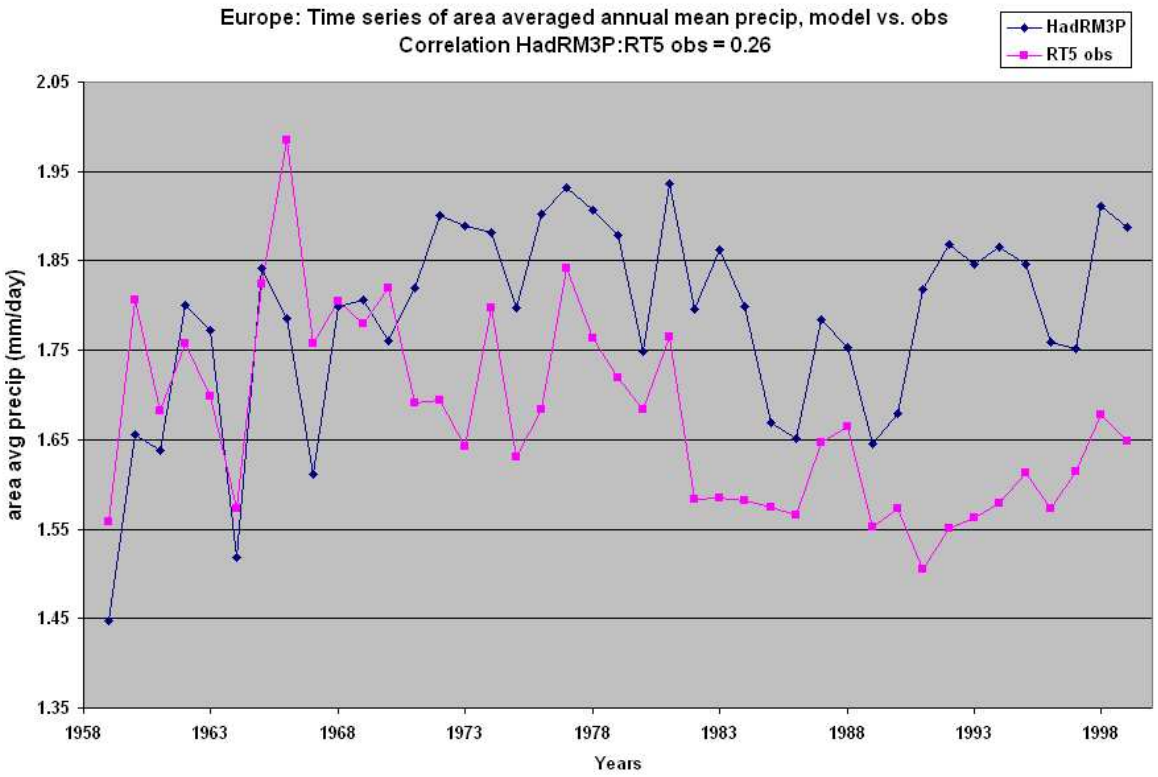

Figure 4.7: Area average annual mean precipitation over Europe, 1959-1999

It is useful as well to examine how well the model is doing on an annual and season basis for individual years and seasons. The time series plots in Figures 4.7 and 4.8 show area average precipitation of the model (violet line) plotted against area average precipitation of the observations for annual mean (Figure 4.7) and seasonal mean precipitation (Figure 4.8). For area average annual mean, the model is observed to slightly exceed the observations. The slight increasing trend seen after approximately 1980 in the model may be due to the advent of satellite remote sensing providing more thorough constraint on the ERA-40 driving data. More information is revealed in the seasonal mean plot, which shows the model is not reproducing the seasonal cycle with the same range as observations. The model and observational peaks usually fall in DJF, but the MAM minima in the observations are not present in the model. This provide a two dimensional representation of the wet bias seen in the MAM Seasonal Mean in Table 4.2.

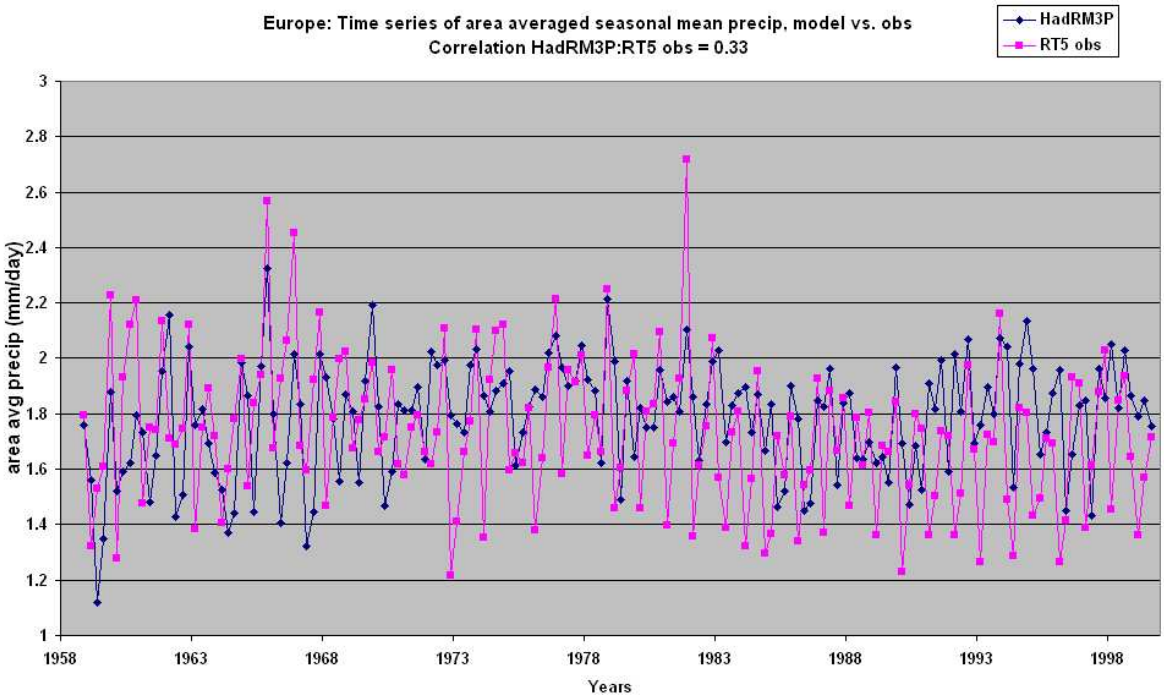

Figure 4.8: Area average seasonal mean precipitation over Europe, Dec 1958 - Dec 1999

4.3.2 Southern Africa

SAF	Seasonal Mean				Wet Day Int				Wet Day Freq			
Seas	Bias	Mn Obs	Bias %	Patt Corr	Bias	Mn Obs	Bias %	Patt Corr	Bias	Mn obs	Bias %	Patt Corr
DJF	1.6	1.6	100	0.82	0.39	4.7	8.4	0.45	0.29	0.31	93	0.71
MAM	0.70	0.89	79	0.64	-.46	4.1	-11	0.04	0.21	0.21	99	0.71
JJA	0.06	0.26	23	0.67	-.84	2.7	-31	0.15	0.06	0.09	69	0.79
SON	1.0	0.85	117	0.82	0.43	3.6	12	0.45	0.21	0.21	97	0.82

Table 4.4: Comparison with model output and Southern African Daily Gridded observational data over Southern Africa for the common period. Values of seasonal mean and wet day intensity are in mm day^{-1}. Values of wet day frequency are unitless.

SAF	Extreme (Non-Pooled)				Extreme (3x3 Pooled)			
Seas	Bias	Mn Obs	Bias %	Patt Corr	Bias	Mn Obs	Bias %	Patt Corr
DJF	9.4	26	36	0.63	6.0	26	24	0.76
MAM	4.0	22	22	0.17	2.8	23	12	0.18
JJA	-6.2	21	-30	0.71	-1.6	18	-8.6	0.54
SON	6.9	23	30	0.28	5.8	21	28	0.69

Table 4.5: Comparison with model output and Southern African Daily Gridded observational data over Southern Africa for the extreme index (with and without spatial pooling). Values in mm day^{-1}.

For **Wet Day Intensity**, the model biases are lower, but the pattern correlation drops to **Poor** quality for all seasons. Figure 4.9 illustrates the cause the 0.04 pattern correlation in MAM. The model's higher intensity events are greatest in the east whereas the observed are greatest in the north and west. The **Wet Day Frequency** pattern for MAM (Figure 4.10) is much better with both the model and the observations (Figure 4.10) showing the east-west gradient of rainfall that is expected in South Africa but the wet day frequencies are considerably higher in the model across the eastern half of the domain. High model biases in Wet Day Frequency are seen in all seasons which clearly are the main contributors to the seasonal mean biases.

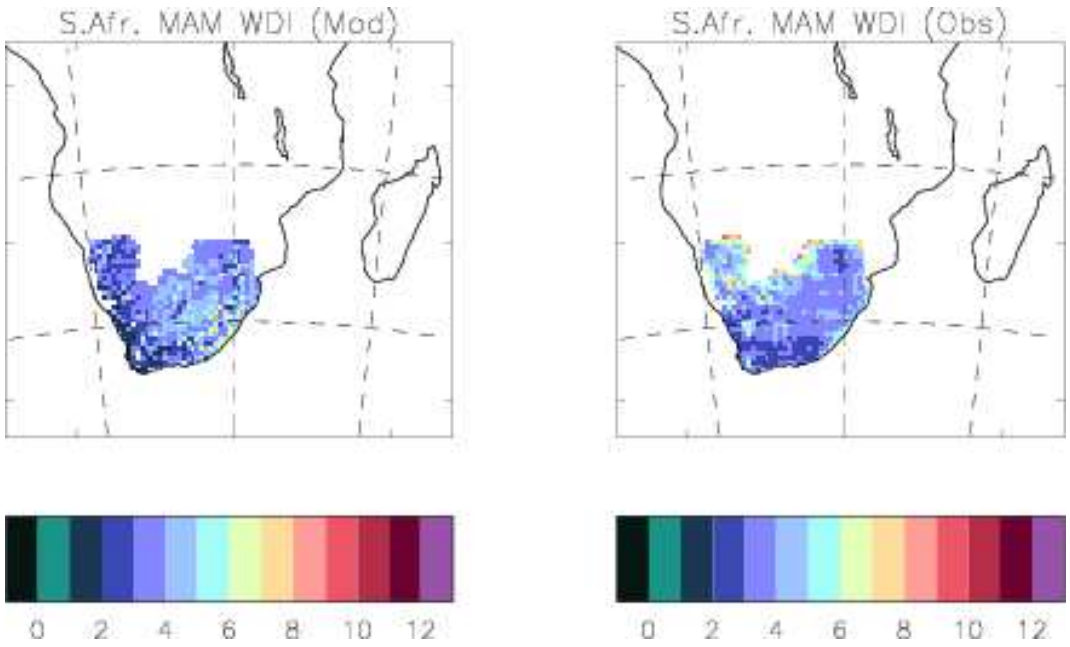

Figure 4.9: Wet day intensity (mm day^{-1}) for Southern Africa, MAM, model (left) and observations (right)

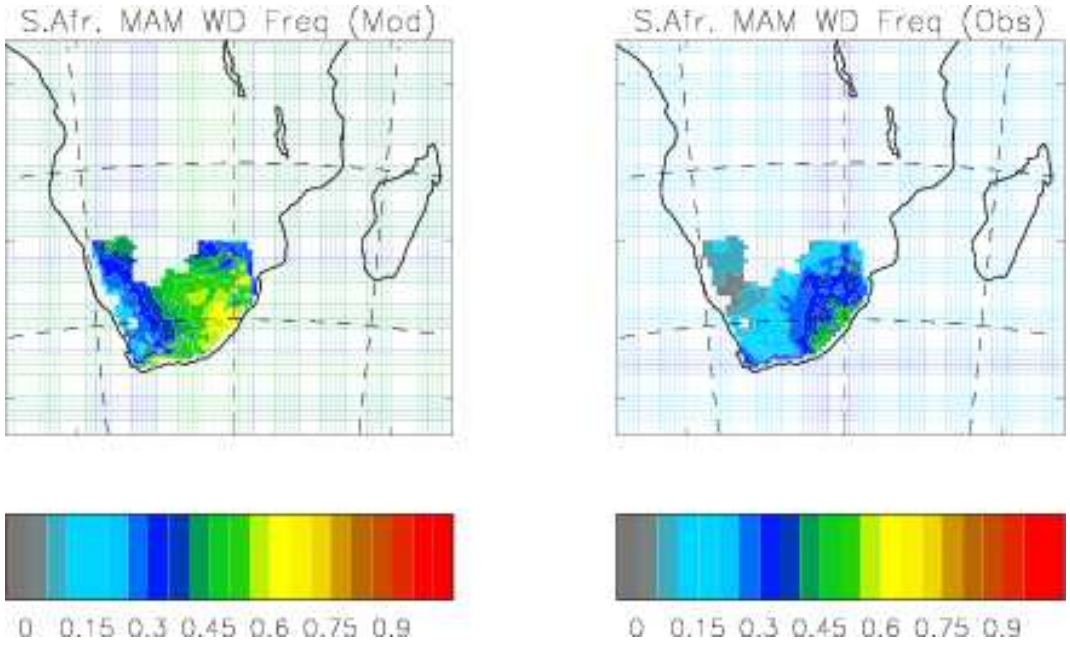

Figure 4.10: Wet day frequency for Southern Africa, MAM, model (left) and observations (right)

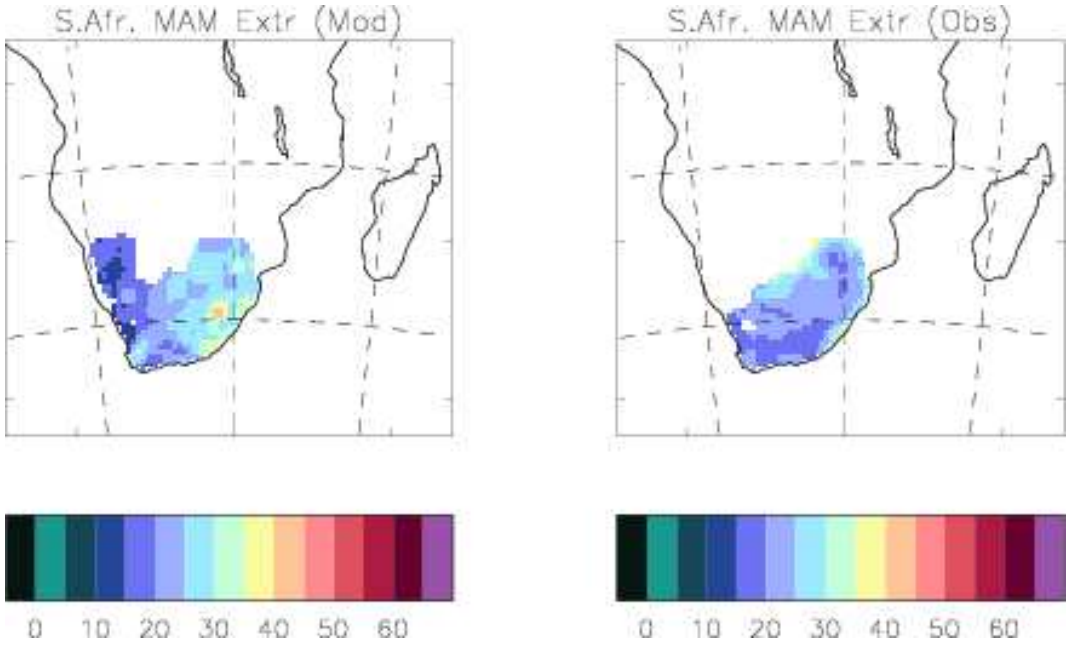

Figure 4.11: Pooled extreme precipitation (mm day^{-1}) for Southern Africa, MAM, model (left) and observations (right)

For the **Extreme** indices in Table 4.5, the 3x3 pooling again generally shows improvement in pattern correlation and decreased model biases with the exception of JJA, in which the pattern correlation is worse. For MAM the model bias is **Good** at only 12%, but the pattern correlation is quite **Poor** implying again that the spatial variability of precipitation intensities is not well captured in this season. In general, the pattern correlations are much higher for the extreme than the mean intensities implying the model is simulating the tail of the distribution better than other parts. The 3x3 pooled extreme precipitation (Figure 4.11) shows the model producing too much extreme precipitation in the east, especially along the eastern coast and over the mountainous country of Lesotho (hearkening back to the orographic rainfall issue described in section 4.3.1). The model does a much better job for 3x3 pooled extreme during DJF (Figure 4.12), correctly simulating the spatial east-west gradient, albeit too wet in the east.

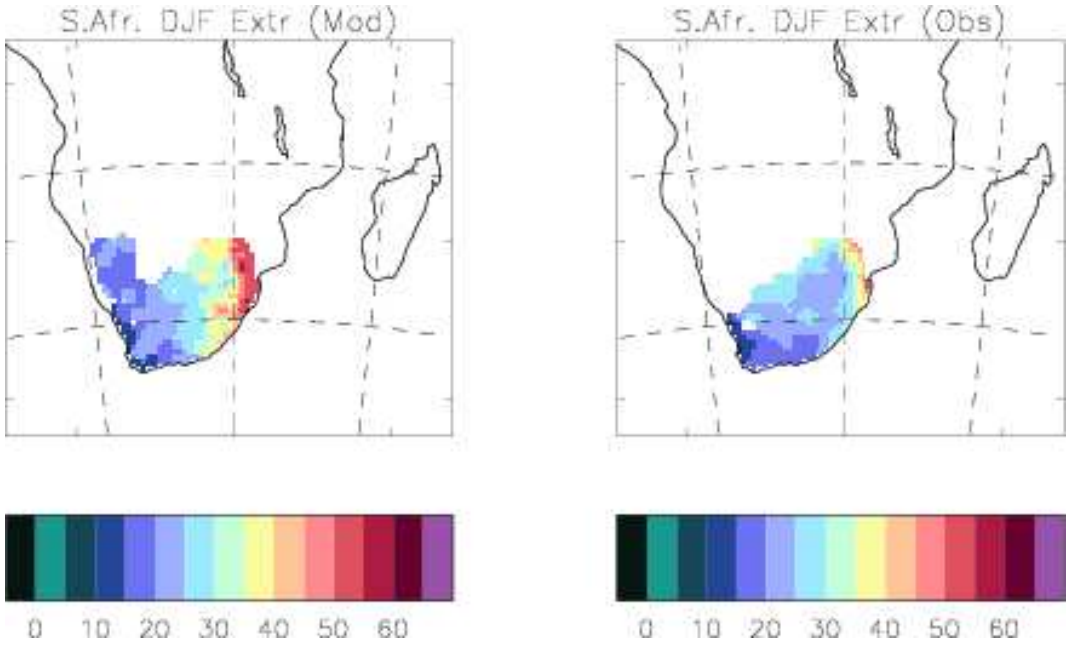

Figure 4.12: Pooled extreme precipitation (mm day^{-1}) for Southern Africa, DJF, model (left) and observations (right)

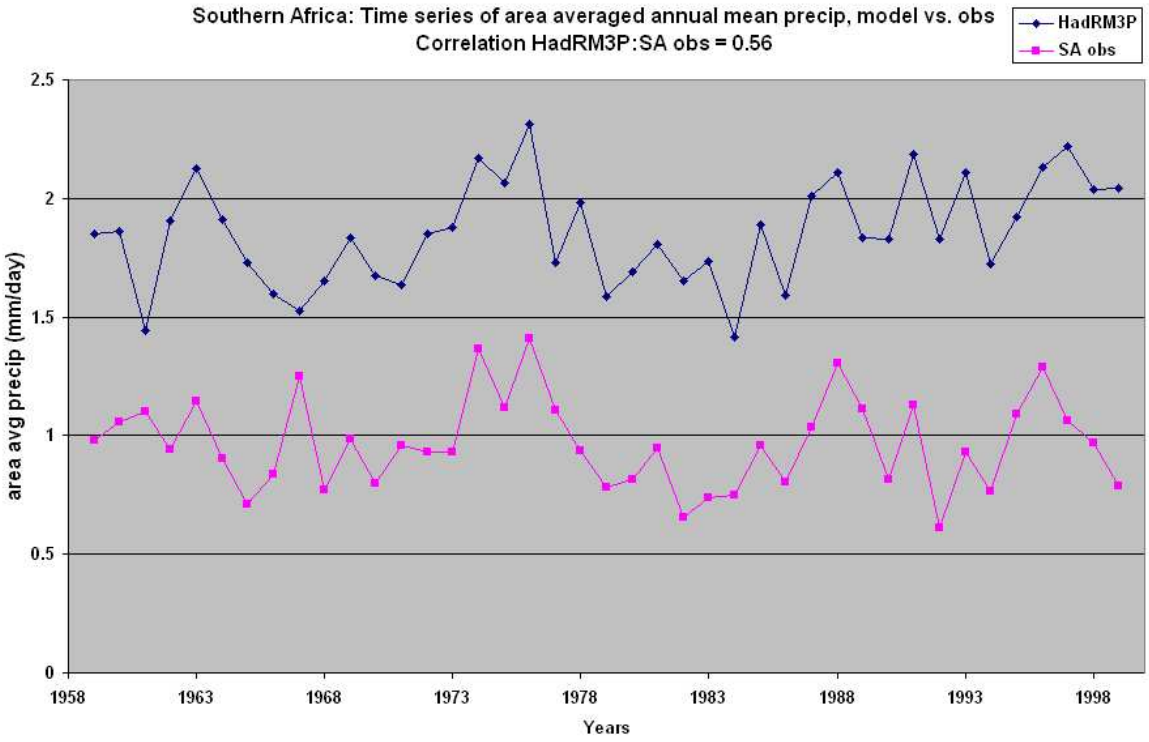

Figure 4.13: Area average annual mean precipitation over Southern Africa, 1959-1999

The area average annual mean and area average seasonal mean time series (Figures 4.13 and 4.14) clearly show that the model has a wet bias versus the observations. The correlations are higher than for Europe, meaning the model is reflecting peak and troughs in the time series of the observations better. Seasonally, the model is peaking (correctly) in the DJF season, but the amount of precipitation the model is producing in DJF is two to three times higher than the observations.

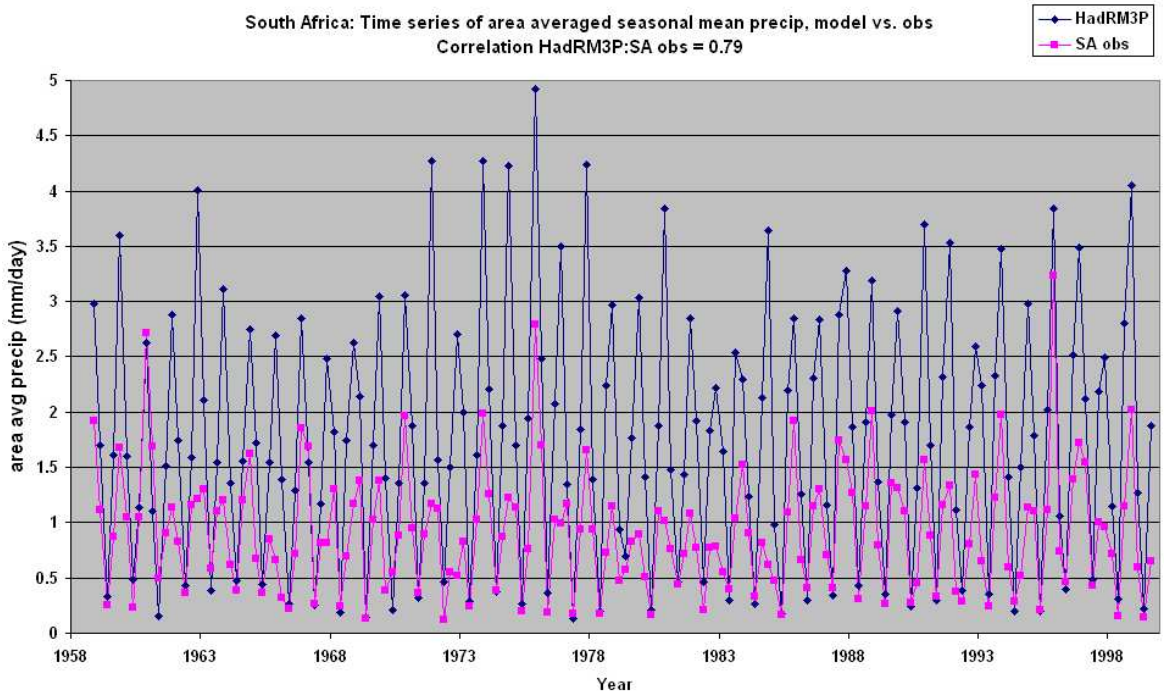

Figure 4.14: Area average seasonal mean precipitation over Southern Africa, Dec 1958 - Dec 1999

4.3.3 Continental USA

USA	Seasonal Mean				Wet Day Int				Wet Day Freq			
Seas	Bias	Mn Obs	Bias %	Patt Corr	Bias	Mn Obs	Bias %	Patt Corr	Bias	Mn obs	Bias %	Patt Corr
DJF	0.44	1.8	25	0.81	0.84	3.9	21	0.85	0.02	0.41	5.9	0.79
MAM	0.58	2.1	28	0.74	0.77	4.5	17	0.78	0.03	0.45	7.5	0.79
JJA	-.03	2.2	-14	0.72	-.55	4.1	-13	0.67	-.02	0.49	-4.2	0.82
SON	-.18	1.9	-9.7	0.71	0.03	4.7	0.66	0.75	-.06	0.39	-14	0.80

Table 4.6: Comparison with model output and UDP observational data over the continental USA for the common period. Values of seasonal mean and wet day intensity are in mm day^{-1}. Values of wet day frequency are unitless.

USA	Extreme (Non-Pooled)				Extreme (3x3 Pooled)			
Seas	Bias	Mn Obs	Bias %	Patt Corr	Bias	Mn Obs	Bias %	Patt Corr
DJF	7.3	25	29	0.89	8.3	24	35	0.92
MAM	6.3	27	23	0.81	6.8	27	25	0.90
JJA	-0.29	26	-1.1	0.56	-1.0	24	-4.2	0.74
SON	4.6	31	15	0.78	4.3	30	14	0.87

Table 4.7: Comparison with model output and UDP observational data over the continental USA for the extreme index (with and without spatial pooling). Values in mm day^{-1}.

The **Seasonal Mean** indices in Table 4.6 all show **Good** pattern correlation with the observations, but there is a slight dry bias in JJA and SON and a wet bias in DJF and MAM. This same pattern holds true for **Wet Day Intensity**, except that the Wet Day SON area average precipitation is improved to within only 1% of the observations. Figure 4.15 shows a plot of Wet Day DJF. Apart from overactive precipitation in the Rockies, Appalachian and Sierra Nevada mountains, the model is seen to reproduce well the spatial patterns of Wet Day Intensity. Figure 4.16 shows JJA Wet Day Intensity, in which the model overestimates precipitation in the northeast and underestimates in the midwest and the southeastern coasts. The midwest is an area of intense summer storm activity brought on by clashing air masses. The model is either not representing the properties and advection of these air masses or not triggering the heavy rainfall properly when they interact. The high observations seen along the southeast coast may be due to tropical cyclones activity which the model is not sufficiently reproducing. In addition to tropical cyclones, these areas experience convective thunderstorms that the model may not be reproducing accurately.

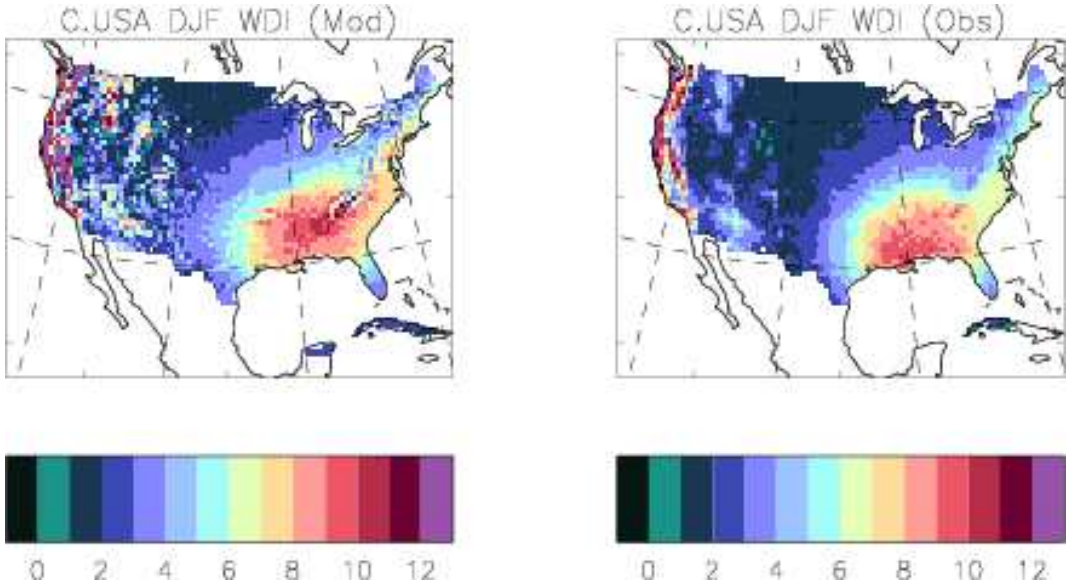

Figure 4.15: Wet day intensity (mm day^{-1}) for the continental USA, DJF, model (left) and observations (right)

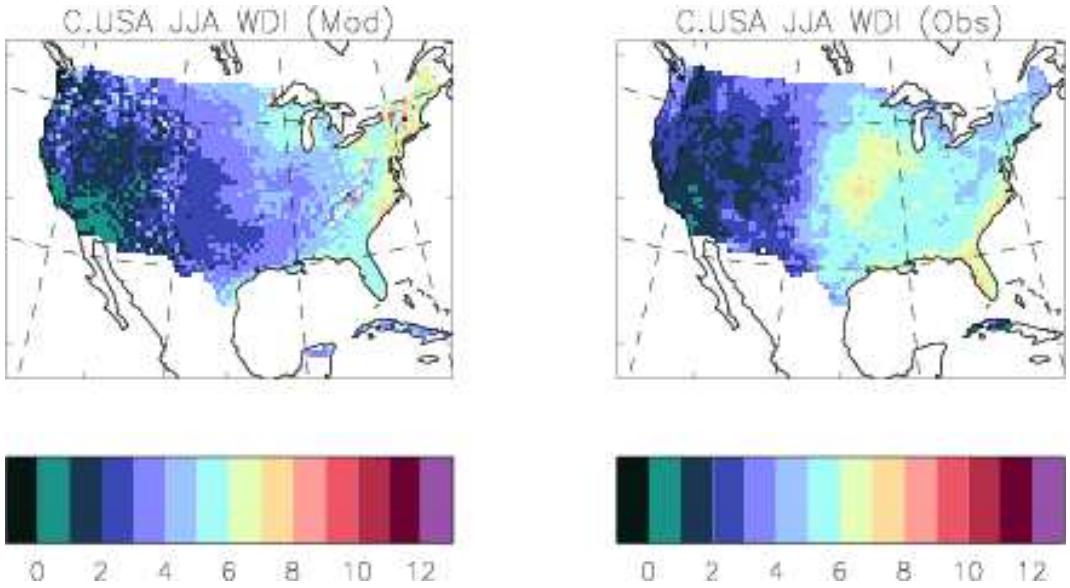

Figure 4.16: Wet day intensity (mm day^{-1}) for the continental USA, JJA, model (left) and observations (right)

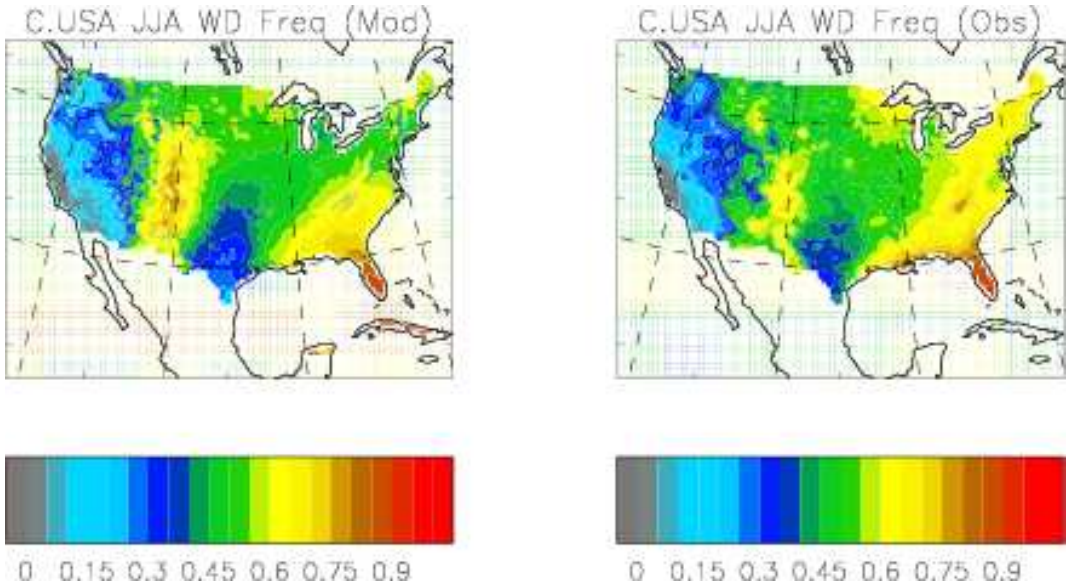

Figure 4.17: Wet day frequency for the continental USA, JJA, model (left) and observations (right)

Wet Day Frequency over the continental USA shows very **Good** performance by the model for pattern correlation and model bias in all seasons. Figure 4.17 is an excellent example of the model capturing both the spatial and the temporal distribution of precipitation of wet days. For the **Extreme** indices in Table 4.7, the spatial pooling again increases the pattern correlation, but, as over Europe, this comes at the cost of increased model bias for the majority of seasons (DJF, MAM, JJA). For the 3x3 pooled JJA extreme (Figure 4.18), there is a slight dry bias and clear underestimation of extreme rainfall in the midwest and southeast coasts consistent with the average intensity results. For 3x3 pooled DJF extreme (Figure 4.19) the model is producing extreme precipitation in nearly the same places as the observations, but has **Fair** performance as far as its bias in that it is too wet over mountainous areas and in the southeast.

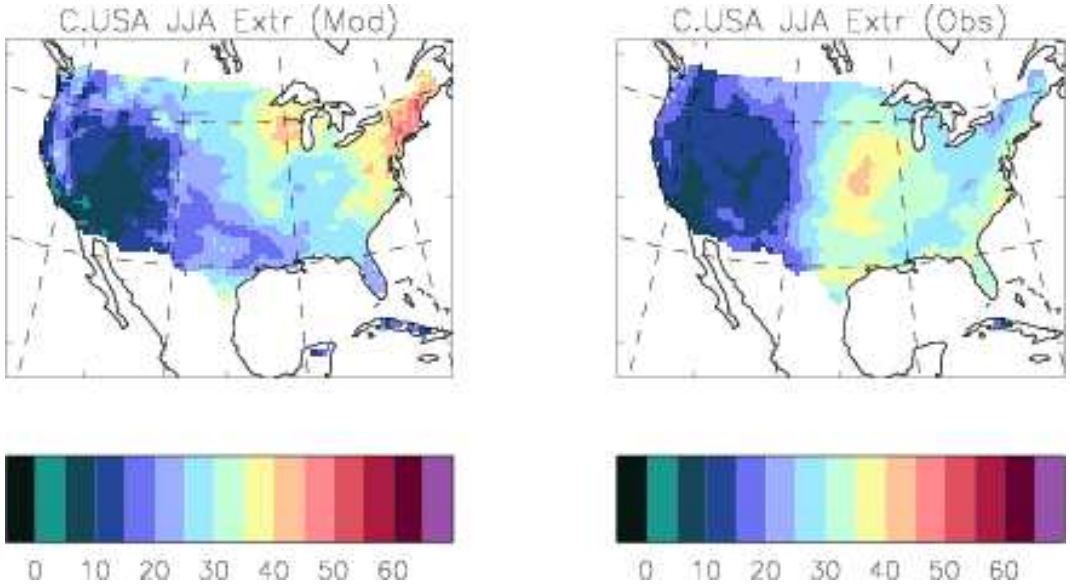

Figure 4.18: Pooled extreme precipitation (mm day^{-1}) for the continental USA, JJA, model (left) and observations (right)

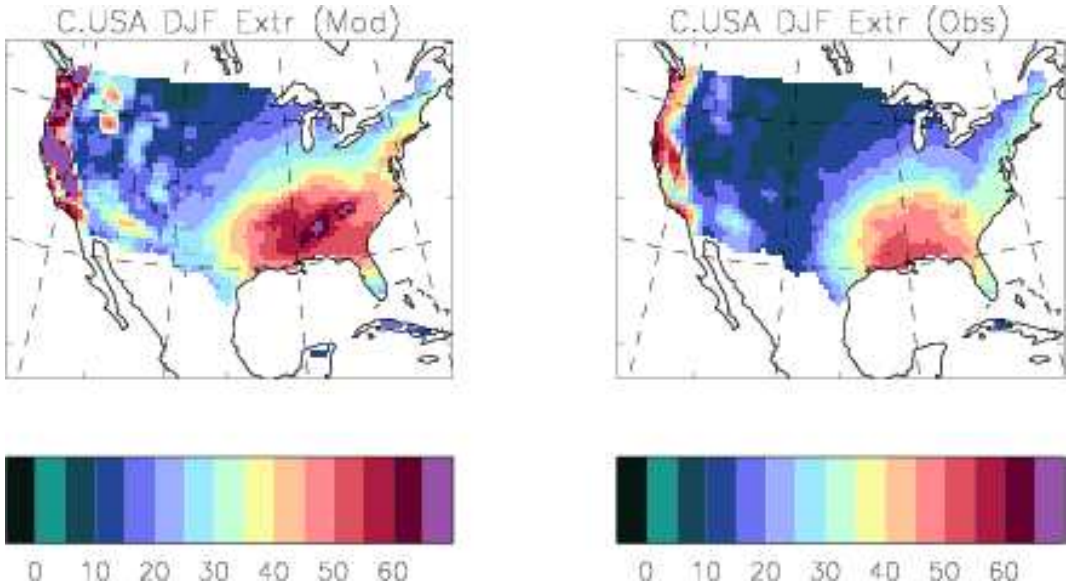

Figure 4.19: Pooled extreme precipitation (mm day^{-1}) for the continental USA, DJF, model (left) and observations (right)

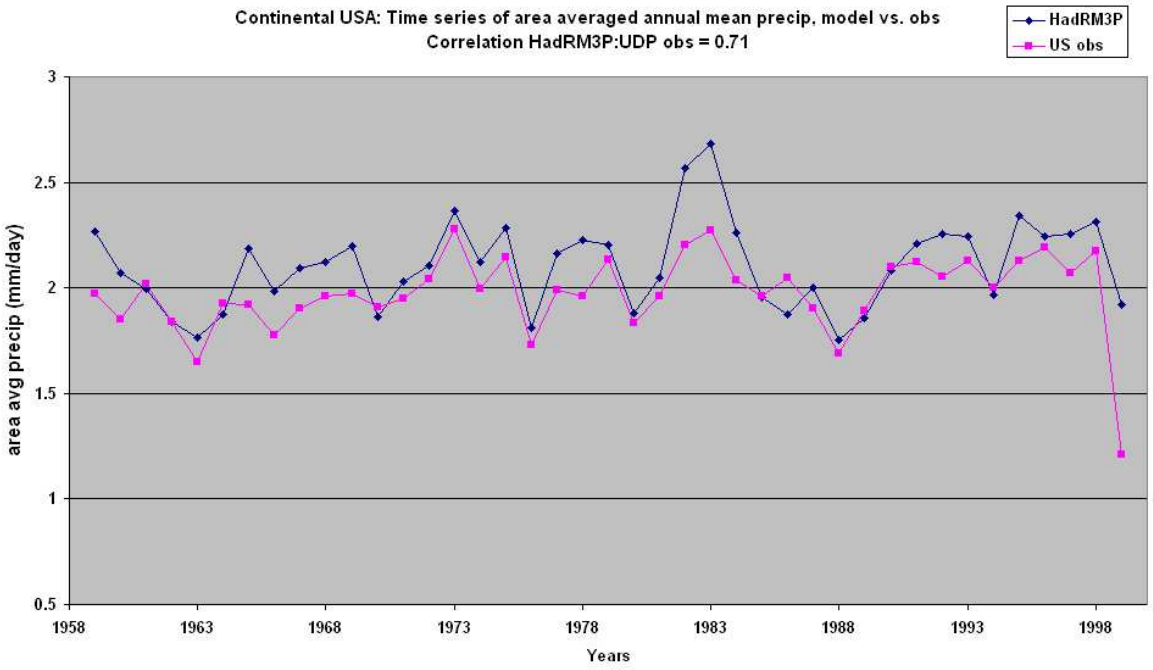

Figure 4.20: Area average annual mean precipitation over the USA, 1959-1999

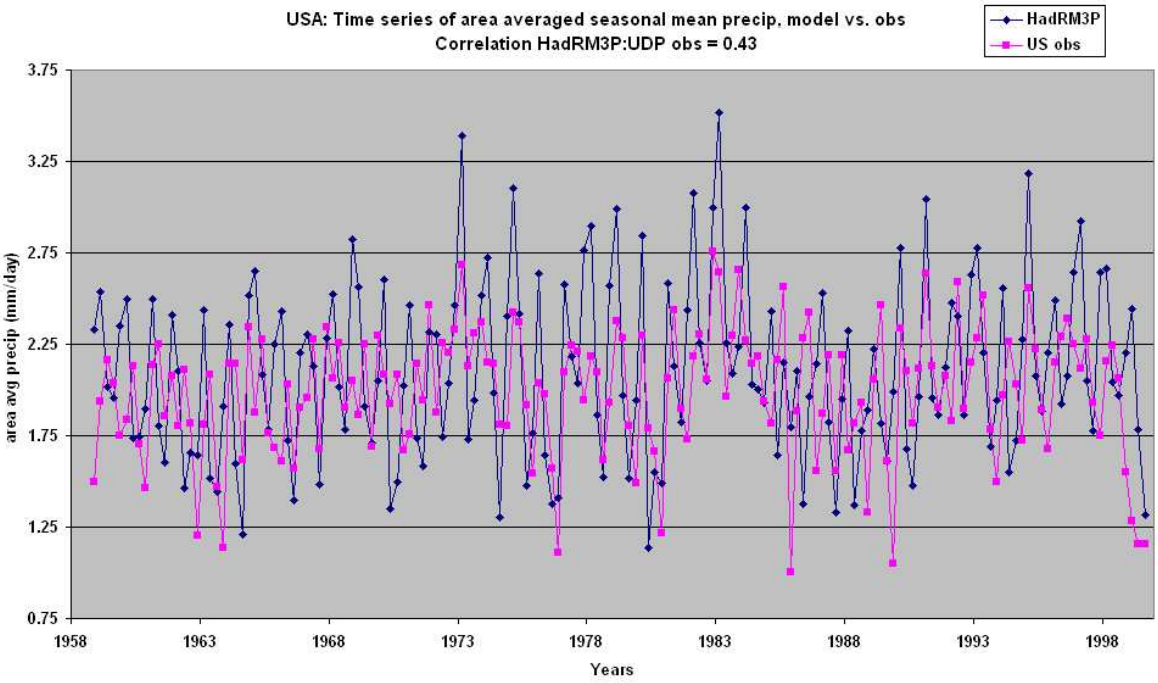

Figure 4.21: Area average seasonal mean precipitation over the USA, Dec 1958 - Dec 1999

The area average annual mean time series (Figure 4.20) shows a high correlation coefficient and general agreement between the plots. The model is thus producing nearly the same amount of precipitation on an annual basis as observations. The agreement is not as good in the area average seasonal mean time series plot (Figure 4.21). The model is reproducing the seasonal cycle, but both DJF and MAM often peak higher than the observations with JJA and SON compensating in that they are often less than observed.

SAS	Seasonal Mean				Wet Day Int				Wet Day Freq			
Seas	Bias	Mn Obs	Bias %	Patt Corr	Bias	Mn Obs	Bias %	Patt Corr	Bias	Mn Obs	Bias %	Patt Corr
DJF	-.03	0.74	-3.6	0.59	-3.6	8.6	-42	0.34	0.03	0.07	45	0.76
MAM	0.99	1.6	62	0.77	-3.4	9.3	-37	0.32	0.08	0.15	52	0.92
JJAS	-.16	7.7	-2.1	0.82	-5.3	15	-36	0.71	0.26	0.48	54	0.79
ON	0.24	1.9	13	0.72	-5.5	12	-45	0.51	0.12	0.14	86	0.87

Table 4.8: Comparison with model output and Indian Daily Gridded observational data over South Asia for the common period. Values of seasonal mean and wet day intensity are in mm day^{-1}. Values of wet day frequency are unitless.

SAS	Extreme (Non-Pooled)				Extreme (3x3 Pooled)			
Seas	Bias	Mn Obs	Bias %	Patt Corr	Bias	Mn Obs	Bias %	Patt Corr
DJF	***	***	***	***	-14	43	-33	0.33
MAM	11	55	19	0.06	-9.7	43	-22	0.59
JJAS	-27	77	-36	0.53	-35	77	-45	0.62
ON	-35	69	-51	0.21	-29	66	-43	0.54

Table 4.9: Comparison with model output and Indian Daily Gridded observational data over South Asia for the extreme index (with and without spatial pooling). Values in mm day^{-1}. *** = insufficient data.

4.3.4 South Asia

The **Seasonal Mean** values in Table 4.8 provide a mixed picture. Arguably the most important season in South Asia is the monsoon (i.e. JJAS). For JJAS, the model's area average precipitation is within only 2% of the observations and has a high pattern correlation (see Figure 4.22). DJF and ON are also close to the observations as far as bias and show **Fair** to **Good** pattern correlation. For MAM, the model shows **Poor** performance in its high model bias which is caused by grossly overestimating rainfall (see Figure 4.23) in eastern India (i.e. the states east of Bangladesh).

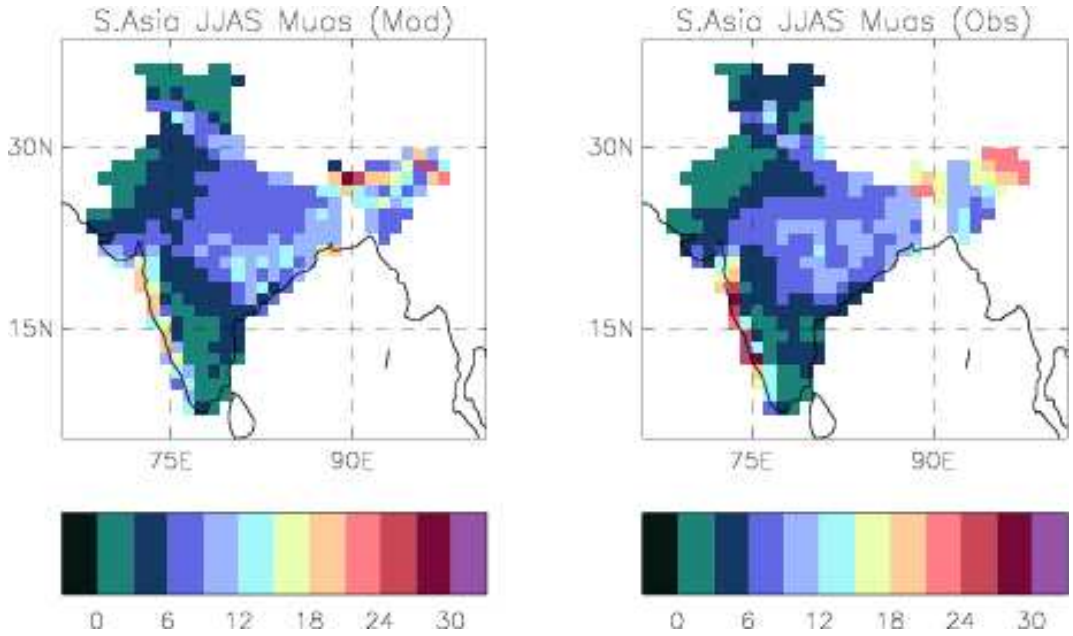

Figure 4.22: Seasonal Mean precipitation (mm day^{-1}) for South Asia, JJAS, model (left) and observations (right)

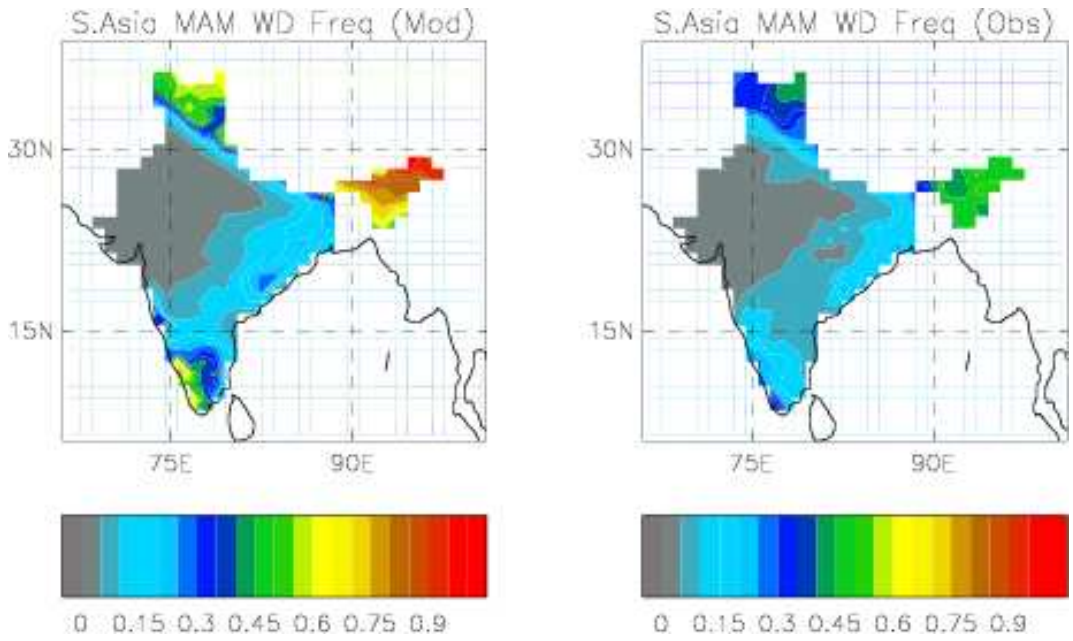

Figure 4.23: Wet day frequency for South Asia, MAM, model (left) and observations (right)

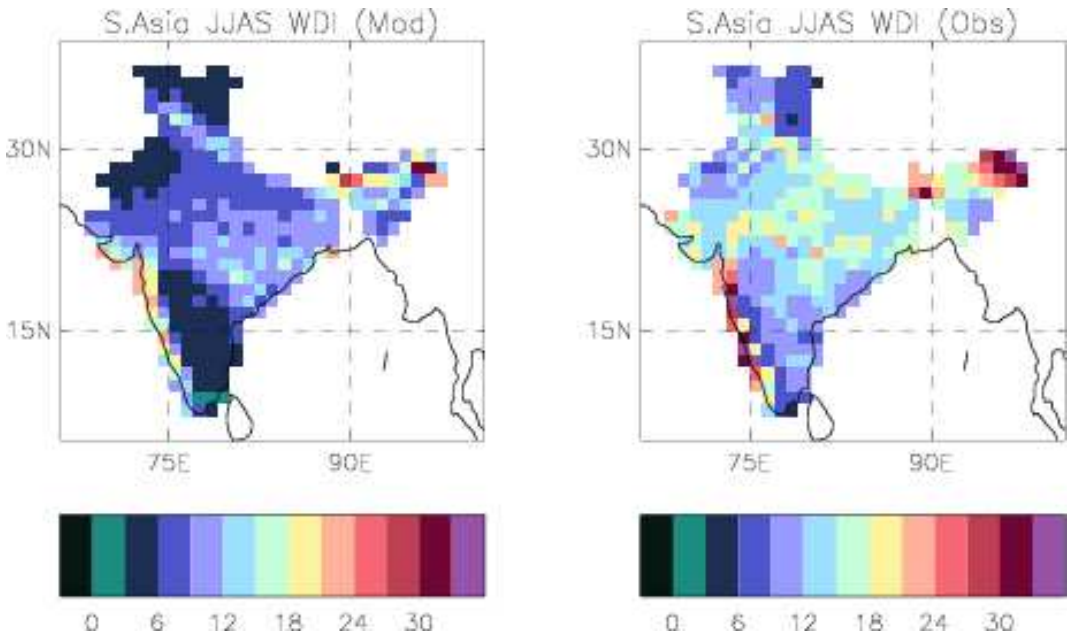

Figure 4.24: Wet day intensity (mm day^{-1}) for South Asia, JJAS, model (left) and observations (right)

Wet Day Intensity in Table 4.8 reveals **Poor** pattern correlation and high model biases for DJF, MAM and ON with a similar bias but better pattern correlation in JJAS (Figure 4.24). For **Wet Day Frequency**, the plot in Figure 4.25 reveals that the model produces precipitation over 60% of the time in all but the northwest, north and a rain shadow area in the south. Again the pattern is reasonable but the frequencies are too high, compensating for the too low average intensity. For MAM wet day frequency (Figure 4.23), the model is producing rainfall too often in eastern India, northern India and the southwest coast. The presence of the Himalayas to the north of India is a possible cause of the poor performance seen in northern and eastern India. Also relevant for these areas is that they are data sparse in the observational data set, which could mean that the data in these areas is not as reliable.

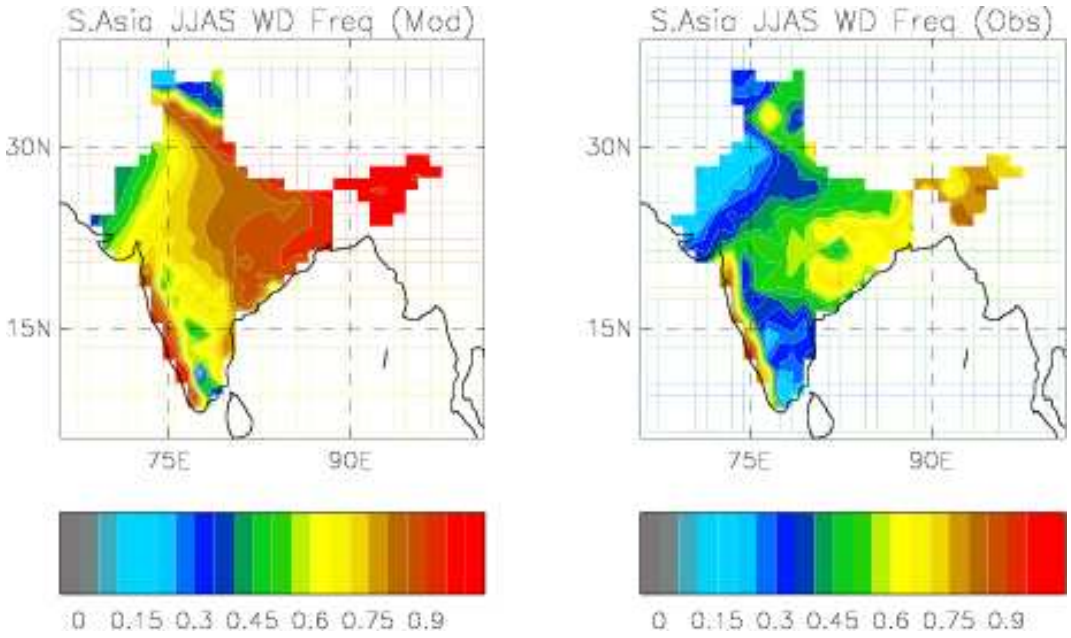

Figure 4.25: Wet day frequency for South Asia, JJAS, model (left) and observations (right)

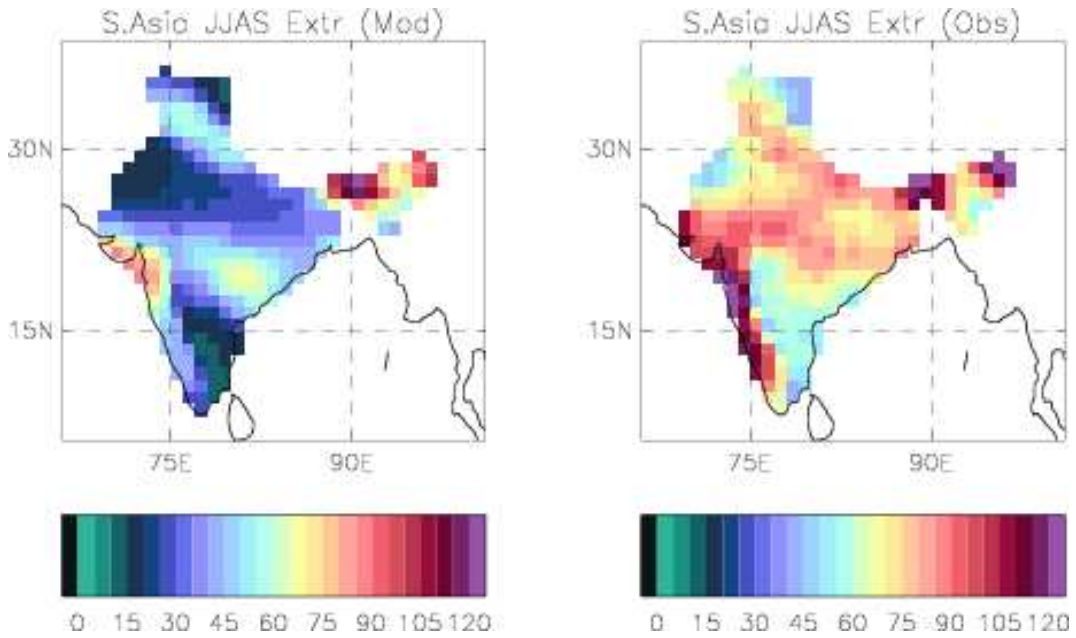

Figure 4.26: Pooled extreme precipitation (mm day^{-1}) for South Asia, JJAS, model (left) and observations (right)

The over-estimated wet day frequencies in the non-monsoon seasons may not be reliable as the significant difference in the mean **Wet Day Intensity** and seasonal mean implies that these results are drawn from a small sample size. Another concern about the representativeness of these results is that the observing station density may be insufficient to capture large area-average (i.e. 1 degree grid–square) light precipitation events. Some evidence for this was provided when the statistics recorded in Table 4.8 were recalculated with a wet day threshold of 0.1 mm. In this case the model biases for the non-monsoon seasons were significantly higher at over 100%.

The **Extremes** in Table 4.9 show marked increases in indices via 3x3 spatial pooling for all seasons. The non-pooled indices do not contain large enough sample sizes to provide reliable information. All seasons show negative biases in extremes which are large in JJAS and ON. Both Figures 4.26 and 4.27 show underestimation of extreme precipitation in everywhere but eastern India. There are two possibilities for the dry bias. One is that the model is not producing enough convective rainfall both spatially and temporally. Another possibility, which may impact on ON especially, is that the observations are taking into account historical tropical cyclones which the model (as with the southeast USA) is not reproducing.

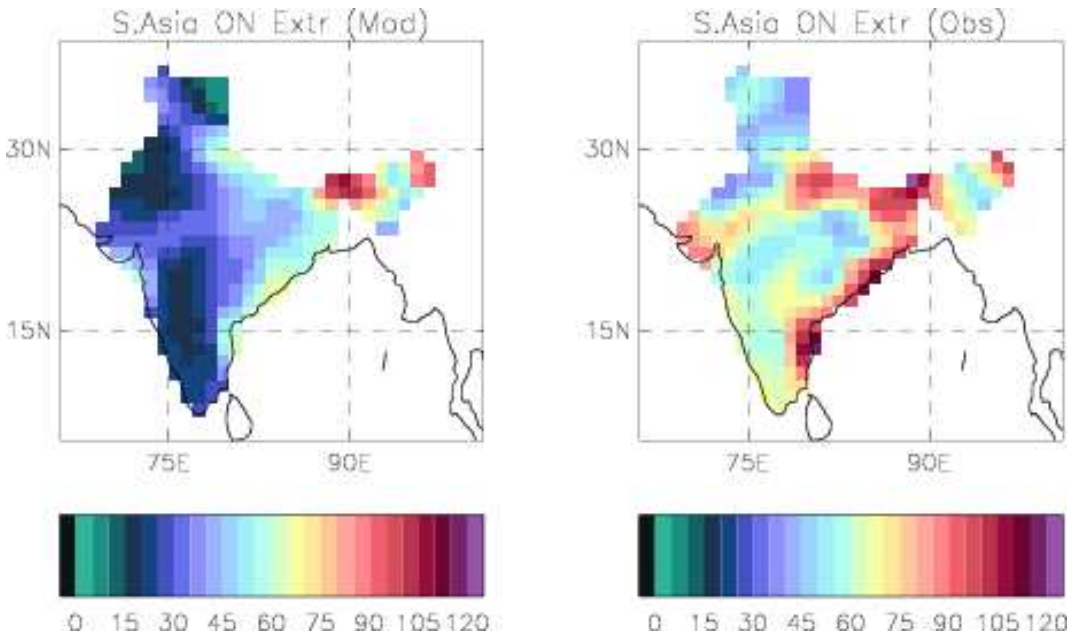

Figure 4.27: Pooled extreme precipitation (mm day^{-1}) for South Asia, ON, model (left) and observations (right)

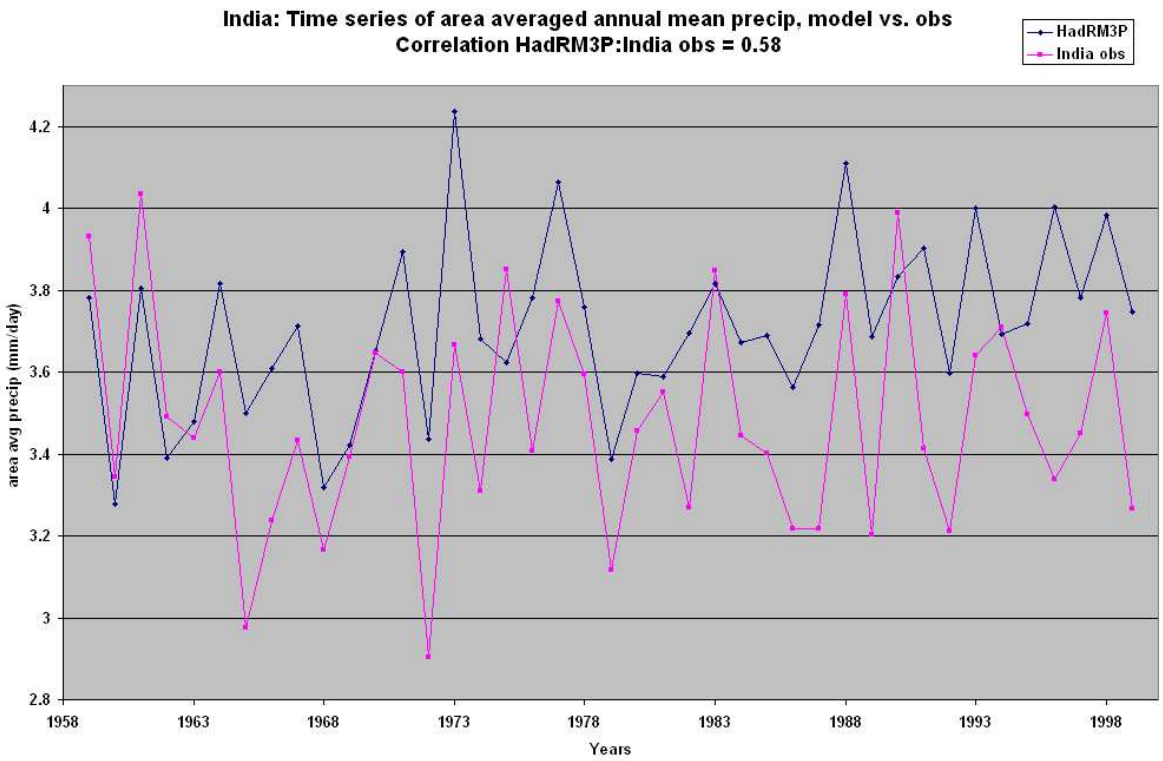

Figure 4.28: Area average annual mean precipitation over India, Dec 1958 - Dec 1999

The area average annual mean time series plot in Figure 4.28 is interesting in that it shows periods of wet and dry years due to natural climate variability. The model is able to follow the wet and dry year patterns in the observations as it is forced by observational re-analysis boundary data in which these patterns appear. The time series of area average model and observational seasonal precipitation (Figure 4.29) shows a 0.98 correlation, meaning the seasonal cycle is very well simulated by the model.

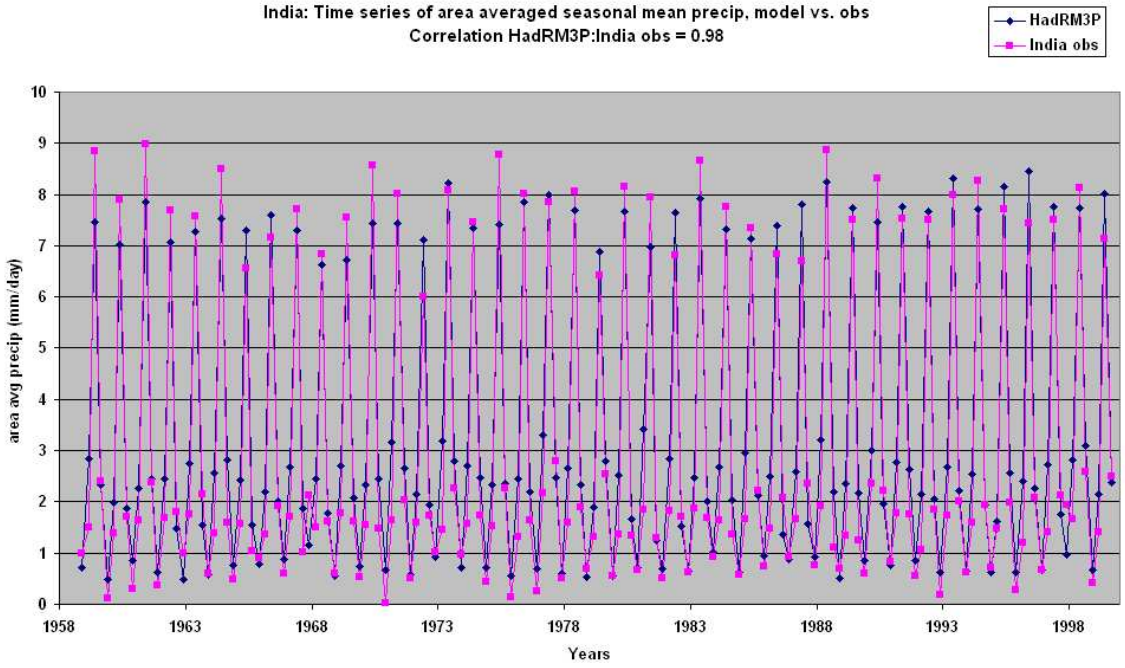

Figure 4.29: Area average seasonal mean precipitation over India, 1959-1999

Chapter 5

Conclusion and Further Work

The HadRM3P regional climate model was run for a 42 year period over four regions with differing climatic processes for rainfall. The results showed better performance spatially and temporally in the representation of extreme precipitation in areas in which large scale precipitation dominates (i.e. the continental United States and Europe) than in areas of in which convective rainfall dominates. In all regions, areas of high orography seemed problematic due to the model producing precipitation in excess of the observations, noting that observational error is generally highest in such areas.

While there are many uncertainties at work in any model validation, the magnitude that the model was underestimating extreme precipitation in India suggests that this warrants further investigation. A more detailed investigation of the observations and further analysis of the precipitation events which the model appears not to be simulating well should be undertaken. Also, re-tuning of the model physics for convection should be considered though the smaller and positive biases in extremes over southern Africa may suggest that underestimation of convective precipitation is not a general problem. If such a tuning were undertaken it could improve model simulation of heavy rainfall in the tropics, while having a minimal effect in extra-tropical areas in which large scale precipitation dominates.

It is important to note, based on the results, that a single index of model performance (e.g. Multiannual Seasonal Mean) can hide a multitude of issues and is therefore insufficient for a thorough model validation. Furthermore, two dimensional indices (such as map plots and time series) provide a fuller picture of how the model is performing.

Further work could be undertaken in relation to this topic. The most obvious is to include more than one set of observations in the comparison in order to establish a "truer" picture of reality to compare to the model performance. Another is to run the model over more regions of the globe. Particularly interesting could be the model's representation of areas experiencing

extreme snowfall, since the model treats rain and snow differently.

In order to further understand the mechanisms contributing to the underestimation of precipitation in South Asia, it would be useful to look at further variables to understand a fuller picture of what is happening in the model. Examining the precipitation identified as solely convective or solely large-scale would also enable discovery of the nature of the total precipitation being produced.

The use of percentiles is only one framework for analysing extreme precipitation. Further work could look at the same data and derive additional useful information using Generalised Extreme Value Theory or other statistical approaches. Dividing the regions into subregions would be another useful action. It is conceivable that the area averaging process undertaken in this study favoured the larger regions more. Creating subregions of relatively equal size would be a way of investigating this hypothesis as well as potentially providing much more local information.

Comparison of model data to observational data at a resolution that is very close is preferable to comparison with quite different resolution. This is due to the loss of some fine scale detail that is a byproduct of the regridding or aggregation. Observations for India at a higher resolution than 1.0° would be especially useful, as 1.0° is fairly coarse compared to the model resolution.

Finally, any or all of the above could be run with another set of re-analysis data driving the model. The NCEP R2 re-analysis data, a data set which has been made use of in a number of studies, is available to drive HadRM3P. Similar model performance when driven by another RCM would either cast further doubt on the model OR could reveal that problems experienced in simulation of extreme precipitation are actually a by-product of unrealistic boundary forcing.

Ultimately the point of this model validation is to establish confidence as to whether HadRM3P is suitable for producing projections of future climate change induced changes in extreme precipitation (cf. 1.4. In the opinion of this author, the answer is yes for areas in which large scale precipitation dominates, and no for the tropics, with the caveat that further work could "overturn" this result. The implications of this mean that the model data may be used (e.g. to drive crop or othet models) with a higher degree of confidence in large-scale precipitation regions than in convective regions.

Only a few indices of model performance have been studied here. A climate model represents many more meteorological phenomena than extreme precipitation, so a reasonable assessment of the full capability of HadRM3P is not possible just by examining one variable. As such, HadRM3P should continue to be run, validated for more variables and improved in its model formulation in the coming days.

Chapter 6

Bibliography

Anderson CJ, Arritt RW, Takle ES, Pan Z, Gutowski Jr. WJ, Otieno FO, da Silva R, Caya D, Christensen JH, Lüthi D, Gaertner MA, Gallardo C, Giorgi F, Hong S-Y, Jones C, Juang H-MH, Katzfey JJ, Lapenta WM, Laprise R, Larson JW, Liston GE, McGregor JL, Pielke Sr. RA, Roads JO, and Taylor JA, 2003. Hydrological processes in regional climate model simulations of the central United States flood of June-July 1993. *J. Hydrometeor.*, **4**, 584-598.

Arnell NW, Hudson DA, and Jones RG, 2003. Climate change scenarios from a regional climate model: Estimating change in runoff in Southern Africa. *J. Geophys. Res.*, **108 (D16)**, 4519-4536.

Ashrit RG, Rupa Kumar K, and Krishna Kumar K, 2001. ENSO-Monsoon relationships in a greenhouse warming scenario. *Geo. Res. Lett.*, **28**, 727-1730.

Association of British Insurers, 2008. The summer floods of 2007: One year on and beyond [online]. London, ABI. Available at: **http://www.abi.org.uk/.**

Bhaskaran B, Jones RG, Murphy JM, and Noguer M, 1996. Simulations of the Indian summer monsoon using a nested regional climate model: domain size experiments. *Climate Dyn.*, **12**, 573-587.

Bhaskaran B, Murphy JM, and Jones RG, 1998. Intraseasonal oscillation in the Indian summer monsoon simulated by global and nested regional climate models. *Mon. Wea. Rev.*, **126**, 3124-3134.

Bromwich DH, and Fogt RL, 2004. Strong trends in the skill of the ERA-40 and NCEP-NCAR reanalyses in the high and midlatitudes of the southern hemisphere, 1958-2001. *J. Clim.*, **17**, 4603-4619.

Buonomo E, Jones RG, Huntingford C, and Hannaford J, 2007. On the robustness of changes

in extreme precipitation over Europe from two high resolution climate change simulations. *Q. J. R. Meteorol. Soc.*, **133**, 65-81.

Chen M, and Xie P, 2008. A global daily gauge-based precipitation analysis, part 1: Assessing Objective Techniques. The 32nd Annual Climate Diagnostics & Prediction Workshop, Oct 22-26, 2007, Tallahassee, Florida, USA.

Crichton D, 2007. The growing risk of climate change on households in England. Proceedings of the AIRMIC Conference, 6 June 2007, Benfield UCL Hazard Research Centre, UCL, London, UK.

Christensen JH, Machenhauer B, Jones RG, Schär C, Ruti PM, Castro M, and Visconti G, 1997. Validation of present-day climate simulations over Europe: LAM simulations with observed boundary conditions. *Climate Dyn.*, **13**, 489-506.

Christensen JH, and Christensen OB, 2003. Severe summertime flooding in Europe. *Nature*, **421**, 805-806.

Christensen JH, Carter TR, Rummukainen M, and Amanatidis G, 2007. Evaluating the performance of regional climate models: The PRUDENCE project. *Clim. Change*, **81**, 1-6.

Christensen JH, Christensen OB, Lenderink G, Rummukainen M, and Jacob D, 2007. ENSEMBLES regional climate modeling: A multi-model approach towards climate change predictions for Europe and elsewhere. American Geophysical Union, Fall Meeting 2007, abstract #GC23B-01.

Christensen OB, Christensen JH, and Botzet M, 2002. Heavy precipitation occurrence in Scandinavia investigated with a Regional Climate Model. In: Climactic Change: Implications for the Hydrological Cycle and for Water Management (Beniston M, ed), 101-112. Kluwer Academic Publishers, the Netherlands.

Dai A, 2005. Precipitation Characteristics in Eighteen Coupled Climate Models. *J. Clim.*, **19** (18), 4605-4630.

Daikaru K, 2006. Dynamic and thermodynamic influences on intensified daily rainfall during the Asian summer monsoon under doubled atmospheric CO2 conditions. *Geo. Res. Lett.*, **33**, L01704.

Dankers R, Christensen OB, Feyen L, Kalas M, and de Roo A, 2007. Evaluation of very high-resolution climate model data for simulating flood hazards in the Upper Danube Basin. Journal of Hydrology, **347**, 319-331.

Denis B, Laprise R, Caya D, and Cote J, 2002. Downscaling ability of one-way nested regional climate models: the Big-Brother experiment. *Climate Dyn.*, **18**, 627-646.

Denis B, Laprise R, and Caya D, 2003. Sensitivity of a regional climate model to the resolution of the lateral boundary conditions. *Climate Dyn.*, **20**, 107-126.

Déqué M, Jones RG, Wild M, Giorgi F, Christensen JH, Hassell DC, Vidale PL, Rockel B, Jacob D, Kjellström E, de Castro M, Kucharski F, and van den Hurk B, 2005. Global high resolution versus limited area model climate change projections over Europe: quantifying confidence level from PRUDENCE results. *Climate Dyn.*, **25**, 653-670.

Done JM, Leung LR, Davis CA, and Kuo B, 2005. Simulation of warm season rainfall using WRF regional climate model. WRF/MM5 User's workshop, June 27-30 2005, Boulder, Colorado, USA.

Easterling DR, Meehl GA, Parmesan C, Changnon SA, Karl TR, and Mearns LO, 2000. Climate Extremes: Observations, Modeling, and Impacts. *Science*, **289**, 2068-2074.

Ebert EE, Damrath U, Wergen W, and Baldwin ME, 2003. The WGNE assessment of short-term quantitative precipitation forecasts. *Bull. Amer. Meteor. Soc.*, **84**, 481-492.

Ebi KL, Mearns LO, and Nyenzi B, 2003. Weather and Climate: Changing Human Exposures. In: Climate Change and Health: Risks and Responses (McMichael AJ, Campbell-Lendrum DH, Corvalan CF, Ebi KL, Githeko A, et al., eds). Geneva, World Health Organisation.

Ekstrom M, Fowler HJ, Kilsby CG, and Jones PD, 2005. New estimates of future changes in extreme rainfall across the UK using regional climate model integrations. 2. Future estimates and use in impact studies. *Journal of Hydrology*, **300**, 234-251.

Evans E, Ashley R, Hall J, Penning-Rowsell E, Saul A, Sayers P, Thorne C, and Watkinson A, 2004. Foresight: Future Flooding. Scientific Summary: Volume I Future Risks and Their Drivers. Office of Science and Technology, London, UK.

Fauchereau N, Trzaska S, Rouault M, and Richard Y, 2003. Rainfall variability and changes in southern Africa during the 20th century in the global warming context. *Nat. Hazards*, **29**, 139-154.

Fowler HJ and Kilsby CG, 2003. Implications of changes in seasonal and annual mean extreme rainfall. *Geophys. Res. Lett.*, **30 (13)**, 1720.

Fowler HJ, Ekstrom M, Kilsby CG, and Jones PD, 2005. New estimates of future changes in extreme rainfall across the UK using regional climate model integrations. 1. Assessment of control climate. *Journal of Hydrology*, **300**, 212-233.

Frei C, Schär C, Lüthi D, and Davies HC, 1998. Heavy precipitation processes in a warmer climate. *Geophys. Res. Let.*, **25**, 1431-1434.

Frei C, and Schär C, 1998. A precipitation climatology of the Alps from high-resolution rain-gauge observations. *Int. J. Clim.*, **18**, 873-900.

Frei C, Christensen JH, Déqué M, Jacob D, Jones RG, and Vidale PL, 2003. Daily precipitation statistics in regional climate models: Evaluation and intercomparison for the European Alps. *J. Geophys. Res.*, **108**, 2287-2306.

Frei C, Schöll R, Fukutome S, Schmidli J, and Vidale PL, 2006. Future change of precipitation extremes in Europe: Intercomparison of scenarios from regional climate models. *J. Geophys. Res.*, **111**, D06105.

Gibson RK, Kållbert P, Uppala S, Hernandez A, Nomura A, and Serrano E, 1997. ERA-15 description. ECMWF Re-Analysis Project Report Series, No. 1, 72pp.

Giorgi F, 1990. Simulation of regional climate using a limited area model nested in a general circulation model. *J. Clim.*, **3**, 941-963.

Giorgi F, and Mearns LO, 1999. Introduction to special section: Regional climate modeling revisited. *J. Geophys. Res.*, **104 (D6)**, 6335-6352.

Gordon C, Cooper CA, Banks H, Gregory JM, Johns TC, Mitchell JFB, and Wood RA, 2000. The simulation of SST, sea ice extents and ocean heat transports in a version of the Hadley Centre coupled model without flux adjustments. *Climate Dyn.*, **16**, 147-168.

Gregory D, and Rowntree PR, 1990. A mass-flux convection scheme with representation of cloud ensemble characteristics and stability dependent closure. *Mon. Wea. Rev.*, **118**, 1483-1506.

Gregory D, and Allen S, 1991. The effect of convective downdraughts upon NWP and climate simulations. In: Ninth conference on numerical weather prediction, 122-123, Denver, Colorado, USA.

Gregory D, Kershaw R, and Inness PM, 1997. Parametrization of momentum transport by convection II: Tests in single column and general circulation models. *Q. J. R. Meteorol. Soc.*, **123**, 1153-1183.

Gregory JM, and Mitchell JFB, 1995. Simulation of daily variability of surface temperature and precipitation over Europe in the current and 2x CO2 climate using the UKMO climate model. *Q. J. R. Meteorol. Soc*, **121**, 1451-1476.

Groisman PY, Knight RW, Easterling DR, Karl TR, Hegerl GC, and Razuvaev VN, 2005. Trends in intense precipitation in the climate record. *J. Clim.*, **18**, 1326-1350.

Hassell DC and Jones RG, 1999. Simulating climactic change of the southern Asian monsoon

using a nested regional climate model (HadRM2). Hadley Centre Technical Note 8, Met Office Hadley Centre, Exeter, UK.

Haylock MR, Cawley GC, Harpham C, Wilby RL, and Goodess CM, 2006. Downscaling heavy precipitation over the United Kingdom: a comparison of dynamical and statistical methods and their future scenarios. *Int. J. Climatol.*, **26** (10), 1397-1415.

Haylock MR, Hofstra N, Klein Tank AMG, Klok EJ, Jones PD, and New M, 2008. A European daily high-resolution gridded dataset of surface temperature and precipitation JGR . (submitted)

Hennesy KJ, Gregory JM, and Mitchell JFB, 1996. Changes in daily precipitation under enchanced greenhouse conditions. *Climate Dyn.*, **13**, 667-680.

Hewitson B, and Crane RG, 2005. Gridded Area-Averaged Daily Precipitation via Conditional Interpolation. *J. Clim.*, **18**, 41-57.

Higgins RW, Shi W, Yarosh E, and Joyce R, 2000. Improved United States Precipitation Quality Control System and Analysis. *NCEP/Climate Prediction Centre ATLAS No. 7.* U. S. DEPARTMENT OF COMMERCE, National Oceanic and Atmospheric Administration, National Weather Service.

Hudson DA, and Jones RG, 2002. Simulations of present-day and future climate over Southern Africa using HadAM3H. Hadley Centre Technical Note 38, Met Office Hadley Centre, Exeter, UK.

Hudson DA, and Jones RG, 2002. Regional climate model simulations of present-day and future climates of Southern Africa. Hadley Centre Technical Note 39, Met Office Hadley Centre, Exeter, UK.

Huntingford C, Jones RG, Prudhomme C, Lamb R, Gash JHC, and Jones DA, 2004. Regional climate model predictions of extreme rainfall for a changing climate. *Q. J. R. Meteorol. Soc.*, **129**, 1607-1621.

Husak GJ, 2006. Developing an Improved Gridded Standardized Precipitation Index for the United States. Eos Trans. AGU, 87(52), Fall Meeting 2006 Suppl., abstract H21B-1377.

Intergovernmental Panel on Climate Change (IPCC), 2000. Special Report on Emissions Scenarios. Nakicenovic N, and Swart R (eds.). Cambridge University Press, UK.

Jacob D, Bärring L, Christensen OB, Christensen JH, Castro M, Déqué M, Giorgi F, Hagemann S, Hirschi M, Jones RG, Kjellström E, Lenderlink G, Rockel B, Sánchez E, Schär C, Seneviratne SI, Somot S, van Ulden A, and van den Hurk B, 2007. An inter-comparison of regional climate models for Europe: model performance in present-day climate. *Clim. Change*, **81**, 31-52.

Jones PD, and Reid PA, 2001. Assessing future change in extreme precipitation over Britain using regional climate model integrations. *Int. J. Climatol.*, **21**, 1337-1356.

Jones RG, Murphy JM, and Noguer M, 1995. Simulation of climate change over Europe using a nested regional climate model. 1: Assessment of control climate, including sensitivity to location of lateral boundaries. *Q. J. R. Meteorol. Soc.*, **121**, 1413-1449.

Jones RG, Murphy JM, Noguer M, and Keen AB, 1997. Simulation of climate change over Europe using a nested regional climate model. 2. Comparison of driving and regional model responses to a doubling of carbon dioxide. *Q. J. R. Meterol. Soc.*, **123**, 265-292.

Jones RG, Noguer M, Hasell DC, Hudson DA, Wilson SS, Jenkins GJ, and Mitchell JFB, 2004. Generating High Resolution Climate Change Scenarios using PRECIS. Met Office Hadley Centre, Exeter, UK, 40pp, April 2004.

Kalnay E, Kanamitsu M, Kistler R, Collins W, Deaven D, Gandin L, Iredell M, Saha S, White G, Woollen J, Zhu Y, Leetmaa A, Reynolds R, Chelliah M, Ebisuzaki W, Higgins W, Janwiak J, Mo KC, Ropelewski C, Wang J, Jenne R, and Joseph D, 1996. The NCEP/NCAR 40-Year Reanalysis Project. *Bull. Amer. Meteor. Soc.*, **77**, 437-471.

Kanamitsu M, Kanamaru H, Yoshimura K, Cui Y, Juang H, and Ohfuchi W, 2008. Dynamical downscaling of global reanalysis. Proceedings of the Third World Climate Research Programme on Reanalysis, 2008. 28 Jan – 1 Feb 2008, Tokyo, Japan.

Karl TR, and Knight RW, 1998. Secular trends of precipitation amount, frequency and intensity in the United States. *Bulletin of the American Meteorological Society*, **79**, no. 2, 231-241.

Kendon EJ, Rowell DP, Jones RG, and Buonomo E, 2008. Robustness of future changes in local precipitation extremes. *J. Clim.*, **doi:10.1175/2008JCLI2082.1.**

Kiktev D, Sexton DMH, Alexander L, and Folland C, 2003. Comparison of modeled and observed trends in indices of daily climate extremes. *J. Clim.*, **16**, 3560-3571.

Klein Tank AMG, and Können GP, 2003. Trends in indices of daily temperature and precipitation extremes in Europe, 1946-1999. *J. Clim.*, **16**, 3665-3680.

Kottek M, Grieser J, Beck C, Rudolf B, and Rubel F, 2006. World map of the Köppen-Geiger climate classification updated, *Meteorol. Zeitschr.*, **15**(3), 259-263.

Kunkel KE, Andsager K, Xin-Zhong L, Arritt RW, Takle ES, Gutowski Jr. WJ, and Pan Z, 2002. Observations and regional climate model simulations of heavy precipitation events and seasonal anomalies: a comparison. *J. Hydrometeor.*, **3**, 322-334.

Landman WA, Botes S, Goddard L, and Shongwe M, 2005. Assessing the predictability of

extreme rainfall seasons over southern Africa. *Geophys. Res. Lett.*, **32**, L23818.

Laprise R, 2008. Regional Climate Modelling. *Journal of Computational Physics*, **227**, 3461-3666.

Lenderlink G, Buishand A, and van Deursen W, 2007. Estimates of future discharges of the river Rhine using two scenario methodologies: direct versus delta approach. *Hydrol. Earth Syst. Sci.*, **11** (3), 1145-1159.

Leung LR, and Qian Y, 2003. Intercomparison of global reanalyses and regional simulations of cold season water budgets in the western United States. *J. Hydrometeor.*, **4**, 1067-1087.

Leung RL, Qian Y, and Bian X, 2003. Hydroclimate of the Western United States Based on Observations and Regional Climate Simulation of 1981-2000. Part I: Seasonal Statistics. *J. Clim.*, **16**, 1892-1911.

Mason SJ, and Joubert AM, 1994. Simulated changes in extreme rainfall over southern Africa. *Int. J. Climatol.*, **17**, 291-301.

Mason SJ, Waylen PR, Mimmack GM, Rajaratnam B, and Harrison JM, 1999. Changes in extreme rainfall events in South Africa. *Clim. Change*, **41**, 249-257.

Mesinger F, 1981. Horizontal advection schemes of a staggered grid – an enstrophy and energy conserving model. *Mon. Wea. Rev.*, **109**, 467-478.

Murphy JM. Predictions of climate change over Europe using statistical and dynamical downscaling techniques. *Int. J. Climatol.*, **20**, 489-501.

New M, Hewitson B, Stephenson D, Tsiga A, Kruger A, Manhique A, Gomez B, Coelho CAS, Masisi DN, Kululanga E, Mbambalala E, Adesina F, Saleh H, Kanyanga J, Adosi J, Bulane L, Fortunata L, Mdoka M, and Lajoie R, 2006. Evidence of trends in daily climate extremes over Southern and West Africa. *J. Geo. Res.*, **111**, D14102.

Noguer M, Jones RG, and Murphy JM, 1998. Sources of systematic errors in the climatology of a regional climate model over Europe. *Climate Dyn.*, **14**, 691-712.

Parry ML, Canziani OF, Palutikof JP, van der Linden PJ, and Hanson CE (eds), 2007. Climate Change 2007: Impacts, Adaptation and Vulnerability. Contribution of Working Group II to the Fourth Assessment Report of the Intergovernmental Panel on Climate Change. Cambridge University Press, Cambridge, UK.

Prömmel K, Geyer B, Jones JM, and Widmann M, 2008. Analysis of a high-resolution regional climate simulation for alpine temperature: validation and influence of the NAO. *Geophys. Res. Abs.*, **10**, EGU2008-A-02383.

Rajeevan M, Bhate J, Kale JD, and Lal B, 2005. Development of a high resolution daily gridded rainfall data for the Indian region. India Meteorological Department, Met. Monograph Climatology No. 22/2005, pp. 26.

Rajeevan M, Bhate J, Kale JD, Lal B, 2006. A high resolution daily gridded rainfall for the Indian region : analysis of break and active monsoon spells, 2006. *Current Science*, **91**, 296-306.

Roy SS, and Balling RC, 2004. Trends in extreme daily precipitation indices in India. *Int. J. Climatol.*, **24**, 457-466.

Salzmann N, Frei C, Vidale PL, and Hoelzle M, 2006. The application of regional climate model output for the simulation of high-mountain permafrost scenarios. *Global Planet. Change*, **56**, 118-202.

Semenov VA, and Bengtsson L, 2002. Secular trends in daily precipitation characteristics: greenhouse gas simulation with a couple AOGCM. *Climate Dyn.*, **19**, 123-140.

Semmler T, and Jacob D, 2004. Modeling extreme precipitation events – a climate change simulation for Europe. *Global Planet. Change*, **44**, 119-127.

Simmons AJ, and Burridge DM, 1981. An energy and angular momentum conserving finite difference scheme and hybrid coordinates. *Mon. Wea. Rev.*, **109**, 758-766.

Solman SA, Nuñez MN, and Cabré MF, 2008. Regional climate change experiments over southern South America. I: present climate. *Climate Dyn.*, **30**, 533-552.

Suppiah R, and Hennesy KJ, 1998. Trends in total rainfall, heavy rain events and number of dry days in Australia, 1910-1990. *Int. J. Climatol.*, **18**(10), 1141-1164.

Tadross MA, Gutowski Jr. WJ, Hewitson BC, Jack C, and New M, 2006. MM5 simulations of interannual change and the diurnal cycle of southern African regional climate. *Theor. Appl. Climatol.*, **86**, 63-80.

Trenberth KE, Dai A, Rasmussen RM, and Parsons DB, 2003. The changing character of precipitation. *Bull. Amer. Meteor. Soc.*, **84**, 1205-1217.

Uppala SM, Kållberg PW, Simmons AJ, Andrae U, da Costa BV, Fiorino M, Gibson JK, Haseler J, Hernandez A, Kelly GA, Li X, Onogi K, Saarinen S, Sokka N, Allan RP, Andersson E, Arpe K, Balmaseda MA, Beljaars ACM, van de Berg L, Bidlot J, Bormann N, Caires S, Chevallier F, Dethof A, Dragosavac M, Fisher M, Fuentes M, Hagemann S, Hólm E, Hoskins BJ, Isaksen L, Janssen PAEM, Jenne R, McNally AP, Mahfouf J-F, Morcrette J-J, Rayner NA, Saunders RW, Simon P, Sterl A, Trenberth KE, Untch A, Vasiljevic D, Viterbo P, and Woollen J, 2005. The ERA-40 re-analysis. *Q. J. R. Meteorol. Soc.*, **131**, 2961-3012.

Vidale PL, Lüthi D, Frei C, Seneviratne SI, and Schär C, 2003. Predictability and uncertainty in a regional climate model. *J. Geophys. Res.*,**108**, (D18), 4586, doi:10.1029/2002JD002810.

Wilby RL, Wigley TML, Conway D, Jones PD, Hewitson BC, Main J, and Wilks DS, 1998. Statistical downscaling of general circulation model output: A comparison of methods. *Water Resources Research*, **34**, 2995-3008.

Zhu Y, and Toth Z, 2001. Extreme weather events and their probabilistic prediction by the NCEP ensemble forecast system. Preprints, *Symposium on Precipitation Extremes: Prediction, Impact and Responses*, Albuquerque, NM. *Amer. Meteor. Soc.*, CD-ROM, P1.38.